Assessing the Sensitivity of Local Snow Cover to Global Climate Change: A General Method and Its Application to Five Swiss Locations

Dimitrios Gyalistras[1], Mario B. Rohrer[2], Christoph Wahrenberger[2], Daniela Lorenzi[2] & Manfred Schwarb[1,2]

Manuscript submitted to Climate Dynamics[3]

9. May 2005

Abstract

A general method to assess possible changes in local snow cover statistics due to global climate change was tested and applied at five representative Swiss sites located between 1018 and 2540 m. The method combines spatial and temporal downscaling of General Circulation Model (GCM) outputs to the local and hourly space and time scales with a conceptual snow model. Extensive validation experiments showed that the temporal downscaling procedure can be used to accurately reproduce seasonal to decadal variations of the local snow cover based on only 8 monthly input variables related to temperature (T) and precipitation (P). The climatic sensitivity of several snow depth statistics was studied for various combinations of changes in long-term mean T and P, plus two GCM-downscaled climate change scenarios. All simulations showed a general decrease in snow cover. In agreement with observations and earlier modelling studies the highest sensitivities were obtained at the sites ≤ 1600 m and for the melting period in spring. The obtained results can be explained by (i) the dominating, negative effect of a warming in situations where present-day T is close to the freezing point; (ii) the generally negative effect of a decrease in P; and (iii) the increasingly positive effect of an increase in P with decreasing T below the freezing point. It was found that at elevations above ca. 2500 m an increase in winter mean P by 20% could offset the effects of a 4 °C warming, at least for the time from October through March. The long-term mean numbers of days with snow depths above 0, 30 and 50 cm were found to decrease by on average 17, 14 and 11 days per °C increase in November-April mean T. The relative frequencies of years with snow depth exceeding 0, 30 and 50 cm for at least 100 days during the main skiing season were found to decrease by on average 19%, 12% and 9% per °C. The proposed method was found to be flexible, more accurate than similar alternative methods, and capable of providing robust, physically plausible scenarios for possible changes in future snow cover.

---

[1] Climatology and Meteorology, Institute of Geography, University of Berne, Hallerstr. 12, CH-3012 Berne, Switzerland. Phone: +41 (0)78 / 602 54 09; e-mail:gyalistras@climate-impacts.ch

[2] Meteodat GmbH, Technoparkstr. 1, CH-8005 Zurich, Switzerland.

[3] Manuscript available electronically under http://www.climate-impacts.ch/DGGreyLit.html#41.

1. INTRODUCTION

Snow is an important feature of the physical environment of mid-latitude mountain regions such as the European Alps. It affects the climate system by modulating the fluxes of energy and water, it influences the dynamics of glaciers, permafrost and debris, and it is important for the ecology of many plant and animal species. With regard to human activities it affects among other things agriculture, water supply and hydroelectric energy production; it causes avalanches that may endanger humans, settlements and infrastructure; and it presents a major resource for the winter tourism industry by enhancing the aesthetic value of the landscape and providing the basis for many winter sports.

The anticipated changes in the Earth's climate (CUBASCH et al. 2001) are likely to have a strong impact also on the Alpine snow cover. The impact will depend on changes in the large-scale climate forcing (e.g., WANNER et al. 2000, SCHERRER et al. 2004), as well as on possible changes in regional-scale climate processes and feedbacks (e.g., FÖHN 1990, GIORGI et al. 1997). The analysis by LATERNSER & SCHNEEBELI (2003) suggests that snow cover in Switzerland is already reacting to the observed 20th century warming.

Clearly, any further changes in the availability and space-time distribution of snow will have numerous implications and deserve closer consideration. The future development of the Alpine snow cover depends however on basic unknowns, such as the future radiative forcing of the global climate system. Planning for an uncertain future can be based on two major approaches: First, on the assessment of the snow cover's climatic sensitivity, understood as the system's response to unit changes in the statistics of driving weather variables. Second, on the construction of quantitative snow cover scenarios. Scenarios are no predictions, but rather consistent descriptions of possible futures that could occur if particular key assumptions, such as specific changes in global and regional climate patterns, would become true.

Sensitivities and scenarios for the snow cover in the European Alps have been studied based on climatological reasoning (FÖHN 1990), statistical analyses of observations (KOCH & RUDEL 1990, BREILING & CHARAMZA 1999, HANTEL et al. 2000, BENISTON et al. 2003a, WIELKE et al. 2004), and simulation models (BULTOT et al. 1992 and 1994, BRAUN et al. 1994, BAUMGARTNER & RANGO 1995, SCHULLA 1997, MARTIN et al. 1997, EHRLER 1998, STADLER et al. 1998, BENISTON et al. 2003b, JASPER et al. 2004). These studies suggested a high sensitivity of the Alpine snow cover to warming; they generally identified the largest sensitivities at elevations below 1500-2000 m, and in the spring season; and they provided some quantitative estimates of possible future changes in the region's snow climatology. However, several problems and open questions still remain:

First, most of the above studies have attempted to quantify possible changes but for a few selected snow cover statistics, such as the average length of the period with snow lying on the ground, or the annual mean water equivalent or depth of the snow cover. Exceptions are the studies by BULTOT et al. (1994) and SCHULLA (1997) that provided some information on possible changes in the numbers of days during the main skiing season (December to April) where snow depth exceeds a given threshold (e.g., 30 cm).

Second, most existing studies have considered only possible changes in long-term mean conditions. However, for many applications possible changes in the seasonal, interannual, or decadal-scale variability of the snow cover are considered to be at least as important as changes in the mean. For instance, ABEGG (1996) and BÜRKI (2000) argue that the winter tourism industry depends more sensitively on the frequency and regularity of "good" and "bad" years for skiing than on long-term average conditions.

Third, most studies have investigated but a limited range of possible future changes in climate. An exception is the study by JASPER et al (2004) that considered 23 different climate change scenarios. Although this work dealt only marginally with snow cover it clearly suggested a high sensitivity of the projected changes to the choice of climate change scenario. A similar result was reported by MARTIN et al. (1997). On the other hand, STADLER et al. (1998) reported very similar snow cover responses to two strongly differing climate change scenarios. To our knowledge, the role of uncertainty in the driving climate scenarios has not been investigated in much detail to date.

Finally, a basic problem occurs due to conflicting requirements related to the physical consistency, robustness and spatio-temporal resolution that can be attained in sensitivity or scenario studies. Statistical models that link observed spatial or temporal climate variations to variations of the snow cover can be considered very robust if they have be based on a large data base that covers a wide range of situations (e.g., HANTEL et al. 2000). However, such models can only be expected to accurately predict averages over larger areas and/or longer time periods, at best, and this contrasts with the needs of many applications. Very detailed information can in principle be obtained from simulations with dynamic snow models that may include very sophisticated representations of snow physics and radiation processes (e.g., ETCHEVERS et al. 2004). Simulation studies are however typically limited by their demanding needs for meteorological input data at a daily or even hourly time step. Moreover, the question arises how the high-frequent weather variability should be included in the driving weather scenarios, and how this variability affects the robustness of the resulting projections.

In this work we address the above problems by presenting, testing and applying a new method that is intermediate between the statistical and physically-based modelling approaches. The method requires only monthly weather data as an input, but we show that it is able to provide physically plausible and robust snow cover scenarios at high spatial and temporal resolutions. As a case study we consider the snow needs of the winter tourism industry at five representative Swiss locations. We explore a wide range of possible changes in key temperature and precipitation parameters, including two regional climate change scenarios that were derived from simulations with two global climate models. We use two older climate model runs, mainly for illustrative purposes. The focus of our study lies in the presentation of the new method and the analysis of the climatic sensitivity of the Swiss snow cover.

In the next section we describe our method and the datasets and models used. Section 3 presents the results of our simulations and compares them to findings from earlier studies. Section 4 povides a discussion of the found sensitivities and of the proposed method. The conclusions of our study are given in Section 5.

2. DATA & METHODS

2.1 Overview

Fig. 1 gives an overview of the proposed method. It employs an array of models and has two main inputs: possible future changes in global radiative forcing agents (Fig. 1, top left), and the needs of impact analysts for snow cover scenarios (bottom right). The main output is given by changes in selected local snow cover statistics (top right). Additional inputs are given by various large-scale and local measurements that are used to calibrate the individual models (Fig. 1, bottom).

The design of our method was based on a series of general considerations that have been discussed in detail by GYALISTRAS et al. (1997) and GYALISTRAS & FISCHLIN (1999). Therefore, here we give only a brief outline of the design rationale. The implementation of the individual steps is presented in more detail in the following subsections. Possible limitations of the method and alternative approaches are discussed later in Section 4.

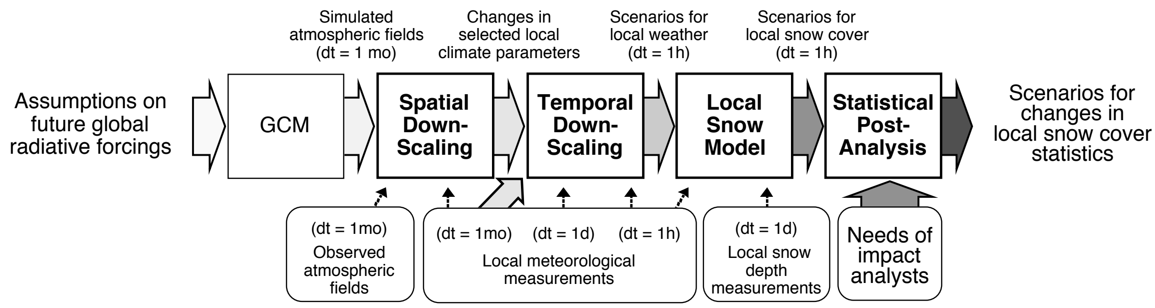

Figure 1: Overview of the procedure used to assess the sensitivity of the local snow cover and to project future scenarios. GCM: General Circulation Climate Model. Arrows: flow of information; top: major procedures/models; bottom: auxiliary data used to determine model parameters; dt = time step.

Following a fairly standard approach to climate scenario construction (MEARNS et al. 2001) the first step of our procedure consists in making available results from scenario runs with General Circulation Climate Models ("GCM", see Fig. 1). The second step deals with the problem that GCMs have a coarse horizontal resolution and thus show only limited skill at spatial scales below several hundreds of km (e.g. VON STORCH, 1995, WIDMANN & BRETHERTON 2000). Therefore a statistical procedure is employed to estimate possible shifts in local climate parameters as a function of the large-scale climatic changes simulated by a given GCM simulation ("Spatial Downscaling"). The third step serves the generation of hourly weather sequences consistent with a given set of present-day or hypothetical future climatic conditions ("Temporal Downscaling"). This step is accomplished with the aid of a stochastic weather generator that is forced by present-day ("control" case) or appropriately perturbed ("scenario" case) monthly weather data. In a fourth step the synthetic hourly weather sequences are used to drive a dynamic simulation model of snow water equivalent and snow depth ("Local Snow Model"). The snow model's results are finally analyzed to derive various statistics, e.g. as required by our winter tourism case study ("Statistical Post-Analysis").

Figure 2: Relief map of Switzerland and location of the five case study sites. Copyright for the relief map by "K606-01©2004 swisstopo".

Table 1: Overview of the case study sites and their climatic conditions

Site	Location	Elevation (m)	T_{win} (°C)	P_{win} (mm)	$Pprob_{win}$ (-)	$N_d(S > 0)$ (-)
Engelberg	Valley floor, Northern Alps	1018	0.7	624	0.52	123
Disentis	Valley floor, Central Alps	1190	1.0	445	0.44	129
Montana	South-facing slope, Central Alps	1495	0.3	575	0.41	139
Davos	Valley floor, Central Alps	1590	-2.2	372	0.42	164
Weissfluhjoch	Mountain peak, Central Alps	2540	-7.1	542	0.53	180

T_{win}, P_{win}, Pprobwin: winter half-year (November-April) mean temperature, total precipitation and average monthly precipitation probability; shown are long-term mean values for the period 1971-1995. $N_d(S > 0)$: long-term mean number of days at which snow depth S exceeds 0 cm in the period Nov. 1 - Apr. 30, winters 1971/72 - 1994/95.

The method was applied to 5 Swiss sites (Fig. 2) that were located at an elevation range between 1018 and 2540 m (Table 1). We chose these sites because of the availability of high-quality, long-term snow data (see below), because they represent the most important climatic regions of the Swiss Alps, and because of their vicinity to important ski tourism destinations.

2.2 Data

2.2.1 Large-scale Data

The fitting of the spatial downscaling models required large-scale (predictors) and local (predictands) weather data. The predictors were given by gridded anomaly fields for monthly mean sea-level pressure (SLP) and monthly mean near-surface temperature

(NST). Both fields had a 5° x 5° latitude/longitude resolution and were defined over the sector 40°E-40°W and 30°N-70°N. We used data for the years 1931-1980, and the anomalies were defined relative to the long-term mean of this period. The SLP data were those by Trenberth & Paolino (1980). For NST we used the data set by Jones & Briffa (1992) and Briffa & Jones (1993). A newer data set would have been available for NST, but for the sector and period considered it would probably differ only little from the one used here (see Jones & Moberg 2003).

For the generation of the local climate change scenarios we considered simulations with two GCMs, the ECHAM1/LSG model of the Max Planck Institute for Meteorology, Hamburg, and the GCMII model of the Canadian Climate Centre (CCC), respectively. The large-scale SLP and NST input fields to the spatial downscaling procedure were determined as follows: For the ECHAM model we used anomalies from a 100 year "2xCO2" (720 ppmv) simulation relative to the 40-year mean of a "1xCO2" (344 ppmv) simulation (Cubasch et al. 1992). For the CCC model we used anomalies for 5 simulated years under 660 ppmv (Boer et al. 1992) relative to the mean from 5 years under 330 ppmv (McFarlane et al. 1992).

Newer GCM simulations (see Cubasch et al. 2001 for an overview) would have been available for the present study. We chose to use these older runs for several reasons. Firstly, we wanted our snow cover scenarios to be consistent with earlier Swiss studies that have investigated climatic impacts on grasslands (Riedo et al. 1997, 1999), forests (Fischlin & Gyalistras 1997) and hydrology (Schulla 1997, Stadler et al. 1998) using the same GCM simulations. Secondly, we wanted to profit from earlier experience (Gyalistras et al. 1994, 1997, 1998) with the two GCMs. Third, as is shown later (Section 3), the two sets of downscaled scenarios showed some interesting differences. Finally, these older GCM runs sufficed for our purposes, since we were mainly interested in method development and the exploration of sensitivities rather than in deriving the "best" currently possible projections for future snow cover.

2.2.2 Local Data

Long-term (≥ 25 years) time series of monthly weather statistics up to the year 1995 were used at the five case study sites in order to fit the spatial downscaling models, to interpolate climate change scenarios across sites, and to drive the temporal downscaling procedure. All needed monthly weather data were derived from daily local temperature and precipitation measurements that were extracted from the "KLIMA" data base of the Swiss Federal Office for Meteorology (MeteoSwiss).

Spatial downscaling was applied to 22 monthly weather statistics related to temperature (T), precipitation (P), global radiation (GR), vapour pressure (VP) and wind speed (WS) (see Gyalistras et al. 1997). However, only the following 8 variables mattered for the snow simulations and will be addressed in more detail in the present study: the monthly total P, the monthly P probability (Pprob; estimated by the relative frequency of the days with daily precipitation ≥ 1 mm), and the monthly mean and within-month standard deviation of daily mean, minimum and maximum T.

For the fitting of the temporal downscaling procedure we used at each site 5 years (1981-1985) of daily and hourly data, which were extracted from the "ANETZ" database of MeteoSwiss. Details on the data preparation can be found in Gyalistras et al. (1997).

At all 5 case study locations we used 14 years of daily snow depth data to tune the snow model and up to 50 years of additional daily data to test the temporal downscaling/snow model chain. Snow data were taken from the snow database of the Hydrology section of the Institute of Geography, ETH Zurich (ROHRER 1992) and from the snow depth database of MeteoSwiss (WITMER 1986). The snow data were quality checked and cleaned for errors and missing data as described in the above mentioned monographs.

2.3 Spatial Downscaling

Spatial downscaling was based on the method of GYALISTRAS et al. (1994). According to this method we first established multivariate regression models that linked interannual variations of the 22 local monthly weather statistics to simultaneous anomalies of the monthly SLP and NST fields. The use of additional predictor fields related to atmospheric humidity would have been desirable (e.g. CHARLES et al. 1999, BECKMANN & BUISHAND 2002). However, this was not possible because no corresponding GCM data were available as an input for scenario construction.

The regression models were determined from a Canonical Correlation Analysis (CCA, e.g. VON STORCH & ZWIERS 1999) in the space spanned by the first few Empirical Orthogonal Functions (EOFs) of the predictor and predictand variables. We performed CCA for the period 1931-1980 separately for each month and for each of the 3 sites Davos, Montana and Engelberg.

Since CCA is known to depend quite sensitively on the choice of the numbers of used predictor and predictand EOFs we performed for each month and location several CCAs using the first 4 to 10 predictor EOFs and the first 5 to 8 predictand EOFs. These numbers were determined based on a systematic investigation of CCA models that used different numbers of EOFs. The lower numbers where given by the numbers of EOFs at which the found correlations between the predictor and predictand data sets started to level off. The upper numbers were given by the numbers of EOFs that were typically needed to explain ~90% of the total variance in the respective data sets.

In a second step we estimated possible future changes in the local weather statistics by applying the regression models to the GCM-simulated anomaly fields (see previous section). For the predictions we considered for each individual CCA model all canonical modes that showed a squared canonical correlation coefficient ≥ 0.15.

The downscaled climate change scenarios were given by site-specific changes in the long-term mean annual cycles of the monthly weather statistics. The changes were estimated by averaging the downscaled weather anomalies from 100 (ECHAM) or 5 (CCC) years and from all fitted 28 CCA models per site and month. The downscaled signals showed rather jagged annual cycles which were smoothed by assigning to each month the 0.25-1-0.25 weighted average value of the downscaled anomalies from that month and the two neighbouring months.

Due to the lack of long-term local measurements, the spatial downscaling procedure could not be applied to the sites Disentis and Weissfluhjoch. Climate change scenarios at these sites were obtained by interpolating the downscaled changes from the site Davos, which is located at a distance of 77 km from Disentis and ~3 km from Weissfluhjoch, respectively (Fig. 2). Interpolation was done with the aid of linear regression models which were fitted separately for each weather statistic and month. To this purpose we used data for the years 1961-1996 for Disentis and 1971-1996 for Weissfluhjoch.

2.4 Temporal Downscaling

For temporal downscaling we used the method of GYALISTRAS et al. (1997; see also GYALISTRAS & FISCHLIN 1999). The method was implemented with the aid of the local stochastic weather generator WeathGen (version 2.5b). WeathGen simulates hourly weather data conditional on monthly weather inputs in two steps: the first step serves the transition from monthly to daily weather, the second step the transition from daily to hourly weather. A simulated hourly weather sequence is fully determined by (i) the parameters of the assumed stochastic processes (see below); (ii) the monthly weather inputs; and (iii) the initialization of the random number generator incorporated in WeathGen.

The monthly weather was described by 22 variables (monthly total P, Pprob, and the monthly means and within-month standard deviations of GR, and daily mean, minimum and maximum T, VP and WS), the daily weather was described by 11 variables (daily total P, daily mean GR, and daily mean, minimum and maximum T, VP and WS), and the hourly weather by 5 variables (hourly total P and hourly mean GR, T, VP, and WS). For technical reasons we applied temporal downscaling to all above weather variables, but actually only the generated hourly P and T values were used to drive the snow model.

Both transitions, from monthly to daily and from daily to hourly weather, are accomplished in WeathGen based on first-order Markov chain-exponential models to simulate P and first-order auto-regressive models to simulate all other variables conditional on P. To ensure consistency among temporal aggregation levels, WeathGen repeatedly simulates daily (or hourly) weather sequences until the statistics of a simulated sequence for a given month (day) are sufficiently close to the respective monthly (daily) inputs. Once a weather sequence has been accepted it is adjusted such, that its statistics exactly reproduce the prescribed inputs (GYALISTRAS et al. 1997).

WeathGen requires a large number of site- and month-specific stochastic process parameters which were determined separately for each site for the years 1981-1985 and were left unchanged in all simulations. In order to simulate hourly weather data under historical and changed climatic conditions we only perturbed the monthly inputs, as described in Section 2.8.

2.5 Snow Model

The used snow model was based on the model by BRAUN & RENNER (1992) that was adapted to simulate local snow cover at a hourly time step. We chose this higher temporal resolution in order to be able to discriminate more accurately between rain and snow in the simulations.

The modified model requires hourly T and P as inputs and produces the following outputs: hourly values for the total water equivalent of the snow cover (W, in mm), plus snow depth (S, in cm) at 07.00 UTC. The model operates at two time steps, an hourly time step, with index k, and a daily time step, with index q = DIV(k-1, 24) + 1, where

DIV(x, y) denotes the integer division of x by y. The value range of the indices is $1 \leq q \leq q_{max}$ and $1 \leq k \leq 24*q_{max}$ with $q_{max} \leq 335$ (cf. Table 3).

The hourly (W_H) and daily (W_D) values for W were calculated according to

$$W_{H(k)} = W_{s(k)} + W_{l(k)} \qquad \text{(Eq. 1a)}$$

$$W_{D(q)} = W_{H(24(q-1)+1)} \qquad \text{(Eq. 1b)}$$

where W_s and W_l are the solid (snow plus ice) and the liquid water content of the snow cover, respectively (both in mm). These two variables are updated according to:

$$W_{s(k+1)} = \mathrm{MAX}(\ 0,\ W_{s(k)} - A_{(k)} + F_{(k)} + P_{s(k)}\ ) \qquad \text{(Eq. 2a)}$$

$$W_{l(k+1)} = \mathrm{LIM}(\ 0,\ W_{max(k+1)},\ W_{l(k)} + A_{(k)} - F_{(k)} + P_{l(k)}\ ) \qquad \text{(Eq. 2b)}$$

Here A denotes the ablation of the snow cover, F the amount of re-frozen meltwater, P_s the hourly total solid precipitation, W_{max} the maximum water holding capacity of the snow cover, and P_l the hourly total liquid precipitation (all variables in mm); MAX(x, y) is a function that returns the maximum of x and y; and LIM(x, y, z) is a function that limits the value of z to between x and y.

The melting of snow (quantity A) was modelled based on a degree day formula. Although this formula is a rough approximation of the energy balance equation of the melting snow cover, the resulting differences are usually quite small, as stated in WMO (1986). We found that a seasonally varying degree day factor $\alpha_{(d)}$ was best for the sites considered:

$$A_{(k)} = \mathrm{MAX}(\ 0,\ \alpha_{(q)}\,(T_{(k)} - \tau_o)\ \Delta t\ ) \qquad \text{(Eq. 3a)}$$

$$\alpha_{(q)} = \alpha_{min} + 0.5\ (\alpha_{max} - \alpha_{min})\ \left\{1+\mathrm{COS}\left(\frac{2\pi}{364}\,(q + \Delta q - 1)\ \right)\right\} \qquad \text{(Eq. 3b)}$$

T denotes the hourly mean air temperature (in °C), τ_o the air temperature at which melting starts (in °C; here 0 °C), and Δt the time increment per time step (1/24 d). The parameters α_{min} and α_{max} (Table 2) determine the seasonal extrema of α, and Δq is the difference between the day number of the first simulated day (q=1) and the day number of the summer solstice, which was always set to 172, i.e. the 21st of June.

Refreezing of meltwater in the snow cover was simulated as "negative melt" according to:

$$F_{(k)} = \mathrm{MAX}(\ 0,\ \phi\ (\tau_o - T_{(k)})\ \Delta t\ ) \qquad \text{(Eq. 4)}$$

where τ_o and Δt are defined as above, and ϕ is a site-specific parameter (Table 2).

The aggregational state of precipitation was determined using an air temperature divider τ_{crit} (e.g., ROHRER 1989). To compensate for errors in precipitation measurements, representativity of precipitation stations and interception losses, multiplicative correction factors for solid (snowfall) and liquid (rainfall) precipitation were applied:

$$P_{s(k)} = \begin{cases} 0 & \text{if } T_{(k)} > \tau_{crit} \\ \kappa_s P_{(k)} & \text{if } T_{(k)} \leq \tau_{crit} \end{cases} \qquad \text{(Eq. 5a)}$$

$$P_{l(k)} = \begin{cases} \kappa_l P_{(k)} & \text{if } T_{(k)} > \tau_{crit} \\ 0 & \text{if } T_{(k)} \leq \tau_{crit} \end{cases} \qquad \text{(Eq. 5b)}$$

The used parameter values are given in Table 2.

The maximum water holding capacity of the snow cover was computed as

$$W_{max(k+1)} = \eta \, W_{s(k+1)} \qquad \text{(Eq. 6)}$$

where η is again a site-dependent parameter (Table 2).

In order to compute S the model traces the fate of $i = 1..q_{max}$ individual snow layers at a daily time step. The water equivalents of the layers are converted to snow depths based upon a simple settling curve model developed by MARTINEC (1977) and further refined by ROHRER (1992). The layer depths ($H_{i(q)}$, in mm) are updated according to

$$H_{i(q)} = \begin{cases} H_{io}(1+a)^{-\lambda} & \text{if } i \leq q \\ 0 & \text{if } i > q \end{cases} \qquad \text{(Eq. 7a)}$$

$$H_{io} = \text{MAX}(0, \Delta W_i / \rho_o) \qquad \text{(Eq. 7b)}$$

Here the index i denotes the i-th layer, which comes into existence at day $q = i$, but actually matters only if net accumulation had taken place during the last 24 h (MAX function in Eq. 7b); $a = q-i$ is the age of the snow in layer; H_{io} is the layer's initial depth; $\Delta W_i = W_{D(i)} - W_{D(i-1)}$ is the balance of W over the i-th simulated day; and λ and ρ_o are parameters (Table 2). The calibrated values for ρ_o were around 100 kg m^{-3} (Table 2), which compares well with measurements from the Swiss Alps (ROHRER et al. 1994).

The daily snow depth S (in cm) was finally computed based on the current density (D, in kg m^{-3}) of the total snow pack according to

$$S_{(q)} = 100 \, W_{D(q)} / D_{(q)} \qquad \text{(Eq. 8a)}$$

$$D_{(q)} = \frac{\sum_{i=1}^{q} \rho_o H_{io}}{\sum_{i=1}^{q} H_{i(q)}} \qquad \text{(Eq. 8b)}$$

The snow model was found to perform well if tested against independent observations (not shown), but if driven with temporally downscaled hourly data some systematic deviations were found. These were corrected empirically by fitting a scaling factor f according to

$$S'_{(q)} = f\, S_{(q)} \qquad \text{(Eq. 9)}$$

All results presented below actually refer to S', but for the sake of simplicity we will address this variable from here on as S.

Table 2: Site-specific parameters of the snow model and fitted parameter values at the five case study sites

Symbol	Unit	Description	Engelberg	Disentis	Montana	Davos	Weiss-fluhjoch
α_{min}	mm °C^{-1} d^{-1}	Min. value of degree day factor (Dec. 21)	2.35	0.38	1.15	0.325	0.01
α_{max}	mm °C^{-1} d^{-1}	Max. value of degree day factor (June 21)	6.25	4.76	8.45	6.79	5.03
ϕ	mm °C^{-1} d^{-1}	Coefficient of refreezing	2.38	2.09	4.31	2.55	2.32
F	--	Scaling factor for daily snow depths	1.00	1.25	1.24	1.21	1.23
η	--	Maximum rel. water holding capacity of snow	0.01	0.08	0.079	0.065	0.001
κ_s	--	Solid precipitation correction factor	1.88	1.18	1.46	1.235	1.25
κ_l	--	Liquid precipitation correction factor	0.64	1.26	0.74	0.69	0.854
λ	--	Exponential settling term of snow layer depth	0.37	0.38	0.325	0.32	0.3
ρ_o	kg m^{-3}	Density of new-fallen snow	122	88	129	92	99
τ_{crit}	°C	Threshold air temperature	0.41	0.1	0.7	0.2	-0.7

The site-specific parameter values (Table 2) were determined for the 14 winters 1981/82 to 1994/95 based on a comparison with measured daily data for S. This was done in two steps: First we drove the model using hourly measured weather data in order to tune all parameters except f (see Eq. 9). Initial parameter estimates were obtained by applying the automated algorithm of MONRO (1971) to data from the first 7 winters. Then we fine-tuned the parameters based on the remaining winters by visually comparing the simulated and observed $S_{(q)}$. In a second step we drove the model with temporally downscaled monthly data and we determined f based on a visual comparison of the measured and simulated daily time series.

2.6 Statistical Post-Analysis

The following statistics of S were computed: (i) the long-term mean of S for every day of the year; (ii) the number of days (N_d) within a given subperiod (P_i, see Table 3) of the winter season where S exceeds a given threshold (h), denoted as $N_d(S \geq h)$; and (iii) the relative frequency of years where N_d is below or above a given number of days (n_d), $RF[N_d < n_d]$ and $RF[N_d \geq n_d]$, respectively.

The used subperiods P_i are summarized in Table 3. Subperiod P_o presents the maximum period where persistent snow cover can be expected to occur at our case study sites. Subperiod P_1 corresponds to the maximum period for which daily snow depth data were available for model validation. Subperiods P_2 and P_3 were considered because of their relevance for winter tourism in Switzerland.

Table 3: Definition of the subperiods used to calculate snow depth statistics

Symbol	Description	Definition	Length (d)
P_o	Whole winter	Sep. 1 - Jul. 31	334
P_1	Winter half-year	Nov. 1 - Apr. 30	181
P_2	Main skiing season	Dec. 1 - Apr. 15	136
P_3	Christmas holiday	Dec. 20 - Dec. 31	12

Note: the lengths of the subperiods P_o to P_2 refer to non leap years.

The snow depth thresholds considered were h = 0, 10, 20, 30, 40 and 50 cm. We chose these values because depending on the terrain, typically at least 10 to 20 cm are needed for Nordic skiing and 30 to 50 cm for downhill skiing in the Swiss Alps.

The critical numbers of days n_d were chosen based on BÜRKI (2000) who drew upon earlier work by WITMER (1986) and ABEGG (1996). According to BÜRKI a "good" winter for downhill skiing is characterized by $N_d \geq 100$ d during period P_2, whereas winters with $N_d < 40$ d must be considered as "bad" for the winter tourism industry. For subperiod P_3 we chose more or less arbitrarily $n_d = 10$ d.

The absolute (AS) and relative (RS) sensitivities of a snow statistic X to a temperature increase were evaluated according to:

$$AS = \partial X / \partial T_{win} \qquad \text{(Eq. 10)}$$

$$RS = AS / \overline{X} \qquad \text{(Eq. 11)}$$

Here T_{win} is the winter half-year (November-April) long-term mean temperature, and $\overline{X}$ stands for the mean of all X values entering the analysis. The AS was estimated by the slope of the linear regression of X on T_{win}.

Note, RS differs from the relative change per degree warming (Δ_{rel}) that has been used in other studies. The latter is typically defined as $\Delta_{rel} = ((X_{scen}-X_{ctrl})/X_{ctrl})/(T_{scen}-T_{ctrl})$ where "ctrl" stands for present-day "control" and "scen" for "scenario" conditions. If only two data points are considered (e.g., one control and one scenario case) holds the relationship:

$$RS = \Delta_{rel} / (1 + 0.5\ \Delta_{rel}) \qquad \text{(Eq. 12)}$$

We used RS instead of Δ_{rel} because our aim was to estimate the average relative response of X in the vicinity of the working point ($\overline{T}$, $\overline{X}$) based on many different value pairs (T, X), rather than to describe relative departures from a particular starting point (T_{ctrl}, X_{ctrl}). For the comparison with other studies we therefore computed RS from the published results according to Eqs. 11 or 12.

2.7 Model Validation

The testing and validation of each single model involved in our procedure (Fig. 1) was beyond the scope of this work. The strengths and limitations of the two used GCMs have been addressed elsewhere (see GATES et al. 1996 for an overview, VON STORCH et al 1997 for the ECHAM model, and MCFARLANE et al. 1992 for the CCC model).

The spatial downscaling procedure has been validated by GYALISTRAS et al. (1994, 1998) who found limited skill for some downscaled variables. Nevertheless, the procedure was found to yield for both GCMs physically plausible and spatially consistent changes in local climates, as discussed by FISCHLIN & GYALISTRAS (1997) and GYALISTRAS et al. (1997, 1998). The strengths and limitations of the regional climate scenarios are briefly discussed in Section 4.3.

In this work we focused on the validation of the temporal downscaling procedure in combination with the snow model since no such work has been reported so far. The test setup was as follows: the temporal downscaling/snow model chain was driven with measured monthly weather data and the simulated snow depth statistics were then compared with corresponding statistics that were derived from the daily snow measurements.

The comparison was based on independent data from the following winters: 1970/71-1980/81 for Engelberg (n=11), 1961/62-1980/81 for Disentis (n=20), 1951/52-1980/81 for Montana (n=30), 1930/31-1980/81 for Davos (n=51), and 1971/72-1980/81 for Weissfluhjoch (n=10).

2.8 Simulation Experiments

In order to be consistent with the snow depth measurements all simulations started at 07.00 UTC on the first day of period P_o (Table 3). The state variables W_s, W_l and H_i were initialized at the beginning of the first hour (k=q=0) of each simulated winter to zero, i.e. the individual winters were simulated independently from each other.

Since the temporal downscaling procedure incorporates a stochastic component we ran the snow model at least n_{realiz} = 30 times per winter, using the same monthly input data but different initial values for the random number generator within WeathGen. We then analyzed the simulated snow depth data separately for each run and determined the final snow cover statistics by taking averages over the statistics from all runs per winter. The number of 30 realizations was chosen because it was found that from this sample size on the multi-run statistics typically did not change by more than a few percents if an additional realization of the hourly weather was considered. For model validation we used throughout n_{realiz} = 30.

For the sensitivity and scenario experiments we used monthly input data from the following winters: 1971/72 - 1994/95 for Engelberg (n=24), 1961/62 - 1994/95 for Disentis (n=34), 1931/32 - 1994/95 for Montana (n=64), 1901/02-1993/94 for Davos (n=93), and 1971/72 - 1994/95 for Weissfluhjoch (n=24).

In order to be able to compare the results between sites, changes in the long-term mean $N_d(S \geq h)$ were evaluated using only the common subset of winters 1981/82-1994/95 (n =

14). This is not a very large sample, but note that these winters covered a wide range of conditions with abundant snow at the beginning of the 1980s and very little snow in the winters 1987/88 to 1989/90. Moreover, in order to enhance the statistical robustness of our results, in this case we used $n_{realiz} = 100$. For the RF statistics, which depended on annual snow cover indices, we considered all winters for which input data were available and we used $n_{realiz} = 30$.

The effects of a given climatic change scenario were simulated by shifting each element of the monthly time series that were used to drive the temporal downscaling procedure by the same scenario-, month- and location-specific amount. The year-to-year variability of the monthly time series was always left unchanged.

For the systematic study of sensitivities we considered 4 synthetic scenarios which specified seasonally uniform changes by +2 and +4 °C for T and by ±20% for P. These scenarios were named T2Pp, T2Pm, T4Pp and T4Pm, where "p" and "m" stand for plus and minus 20%, respectively. The 8 relevant monthly input variables for the snow simulations were adjusted in these scenarios as follows: the same T increase was applied to the monthly means of daily mean, minimum and maximum T; the within-month standard deviations of the daily T variables were left unchanged; and the assumed change in P was associated with a change of the same sign in Pprob by 10%.

The ECHAM and CCC scenarios specified changes not only for the monthly means, but also for the within-month standard deviations of the T variables (see Section 2.2). The two GCM-based scenarios are presented in more detail in Section 3.2. In order to study the effects of a gradual shift in climate we formulated additional scenarios by scaling all originally downscaled changes by a factor s varying from 0.2 to 2.0 in steps of 0.2. An exception was applied to the within-month standard deviations of daily mean, minimum and maximum T under the CCC scenario. The changes for these three variables were found to be quite large (see later), and in order to restrict them to a plausible value range they were scaled only up to s = 1.0 and then they were kept constant to the originally downscaled values. The resulting scenarios were named ECH-TR(s) and CCC-TR(s), where TR stands for transient climate change.

3. RESULTS

3.1 Validation of the Temporal Downscaling/Snow Model Chain

Fig. 3 shows the measured and simulated long-term mean S at the sites Disentis and Davos. It can be seen that the seasonal development of S was reproduced in the validation period as well as in the fitting period. The simulations yielded a much smoother seasonal cycle than the measurements and tended somewhat to underestimate S. This tendency was smaller at the lowest site, Engelberg, and more pronounced at the highest site, Weissfluhjoch (not shown).

Fig. 4 compares the observed and simulated numbers of days at which S exceeds the 30 cm threshold in period P_1, again using the sites Disentis and Davos as an example. It can be seen that the simulations captured the observed interannual to decadal-scale variability of the S statistics with very good skill.

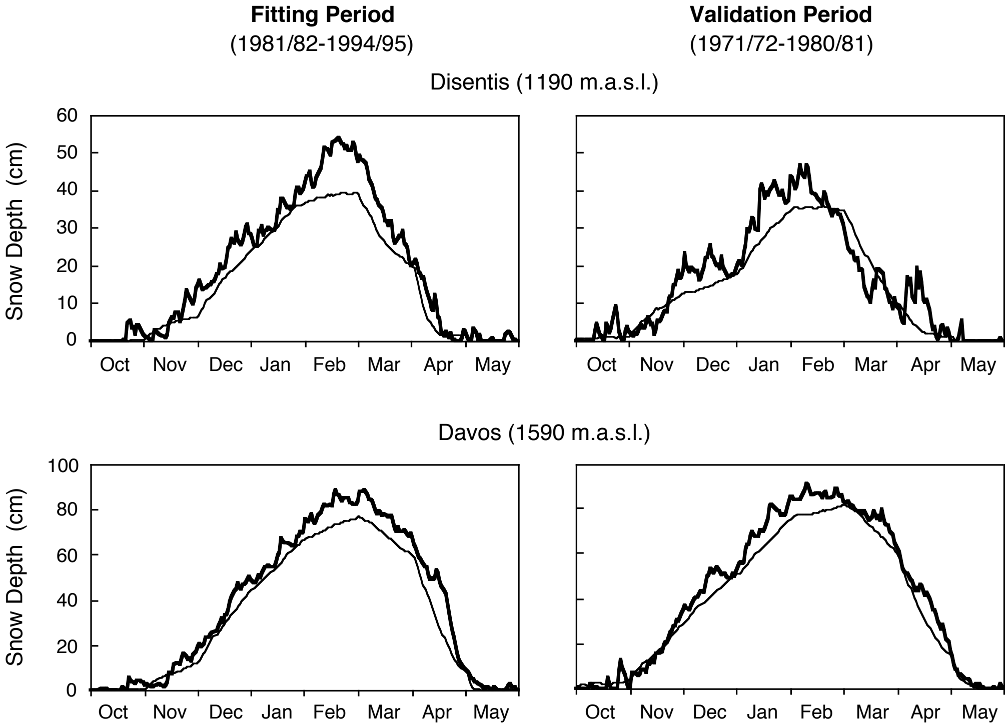

Figure 3: Comparison of measured (thick lines) and simulated (thin lines) long-term mean daily snow depths at Disentis (top) and Davos (bottom).

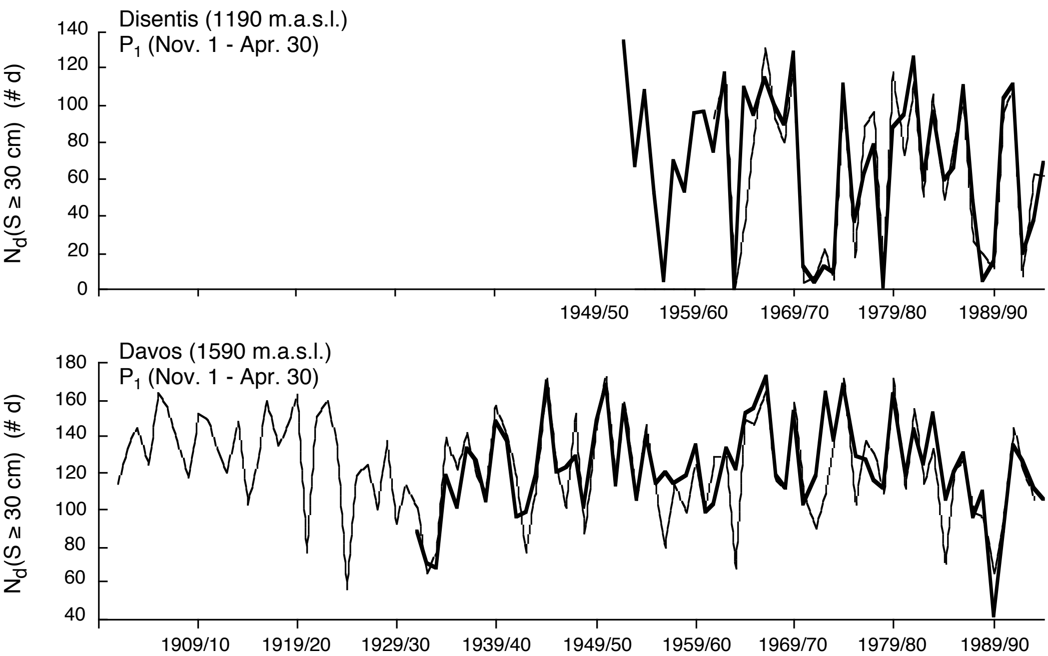

Figure 4: Comparison of measured (thick lines) and simulated (thin lines) numbers of days at which snow depth exceeds 30 cm in subperiod P_1 (Nov. 1 - Apr. 30) at Disentis (top) and Davos (bottom). The parameters of the snow model were fitted for the winters 1981/82-1994/95, those of the temporal downscaling procedure for the years 1981-1985.

Table 4: Validation results for the numbers of days at which snow depth exceeds a given threshold

Site	n	Statistic	P_1 (Nov. 1 - Apr. 30)						P_2 (Dec. 1 - Apr. 15)						P_3 (Dec. 20 - Dec. 31)					
		h	0	10	20	30	40	50	0	10	20	30	40	50	0	10	20	30	40	50
Engelberg	11	r	**.87**	***.53***	**.56**	**.81**	**.87**	**.87**	**.81**	.47	***.53***	**.80**	**.88**	**.88**	**.79**	**.79**	***.53***	**.88**	**.61**	.29
		Δ	3.1	-1.0	2.4	1.6	2.7	0.7	0.5	-2.1	1.0	0.3	1.4	-0.3	0.8	0.0	-0.1	0.1	0.9	0.5
		Δ%	2	-1	4	4	10	4	0	-2	2	1	5	-2	8	1	-1	4	88	131
Disentis	20	r	**.91**	**.92**	**.89**	**.88**	**.87**	**.86**	**.91**	**.91**	**.89**	**.89**	**.88**	**.86**	**.54**	**.76**	**.72**	**.66**	**.86**	**.82**
		Δ	0.7	-1.5	-3.2	-1.8	0.4	-0.5	0.8	-0.9	-3.2	-2.7	-0.5	-1.1	1.4	0.9	-0.3	-0.4	0.1	-0.3
		Δ%	1	-1	-4	-3	1	-1	1	-1	-4	-4	-1	-3	15	11	-4	-8	3	-13
Montana	30	r	**.77**	**.91**	**.88**	**.87**	**.88**	**.88**	**.79**	**.91**	**.86**	**.85**	**.89**	**.89**	**.50**	**.72**	**.65**	**.75**	**.84**	**.78**
		Δ	-4.4	-8.3	-10.5	-11.5	-10.7	-10.1	-6.0	-8.5	-10.4	-11.2	-11.0	-10.7	0.0	-0.6	-0.7	0.1	0.3	0.0
		Δ%	-3	-7	-9	-11	-12	-12	-5	-8	-10	-12	-13	-14	0	-7	-9	1	7	-1
Davos	51	r	**.72**	**.76**	**.75**	**.80**	**.86**	**.90**	**.32**	**.54**	**.61**	**.68**	**.84**	**.89**	NA	.11	**.61**	**.72**	**.88**	**.90**
		Δ	-0.3	-1.9	-2.4	-2.5	-1.7	3.9	-1.4	-1.5	-1.6	-2.3	-2.3	2.8	0.0	0.0	0.2	0.5	0.2	0.9
		Δ%	0	-1	-2	-2	-2	4	-1	-1	-1	-2	-2	3	0	0	2	6	3	23
Weiss-fluhjoch	10	r	(.01)	(.01)	(-.01)	(.00)	**.72**	**.68**	(**.85**)	(.45)	(.35)	(.33)	(.32)	(.01)	NA	NA	NA	NA	NA	NA
		Δ	-1.4	-3.3	-5.5	-7.1	-7.2	-12.6	-0.1	-0.6	-1.1	-1.8	-2.9	-7.0	0.0	0.0	0.0	-0.1	-0.5	-1.8
		Δ%	-1	-2	-3	-4	-4	-7	0	0	-1	-1	-2	-5	0	0	0	-1	-4	-15

n: number of winters considered for validation; r: Pearson product-moment correlation coefficient between the simulated (sim) and the observed (obs) time series of numbers of days within a given subperiod (P_i) of the year at which snow depth exceeds a given threshold h; Δ: mean deviation = $(1/n)\sum(sim_i\text{-}obs_i)$; Δ%: mean relative deviation = $(1/n)\sum[100(sim_i\text{-}obs_i)/obs_i]$; h: snow depth threshold (in cm); P_1-P_3: subperiods of the year considered; NA: statistic not available; ***x***, **x**, and **x** denote r values which are significantly different from zero at the 90%, 95% and 99% confidence levels, respectively (two-tailed test, H_o: r=0). Brackets denote cases where the coefficient of variation of the measured time series is below 5%.

Table 5: Validation results for the relative frequencies of years with selected snow cover characteristics

Site	Statistic	RF[$N_d(S \geq h) < 40$ d] P_2 (Dec. 1 - Apr. 15)						RF[$N_d(S \geq h) \geq 100$ d] P_2 (Dec. 1 - Apr. 15)						RF[$N_d(S \geq h) \geq 10$ d] P_3 (Dec. 20 - Dec. 31)					
	h	0	10	20	30	40	50	0	10	20	30	40	50	0	10	20	30	40	50
Engelberg	RF_{obs}	0	0	36	36	82	91	82	27	9	9	0	0	73	55	27	18	0	0
	RF_{sim}	0	9	36	55	64	91	82	18	9	0	0	0	73	27	18	9	0	0
	Δ	0	9	0	**18**	**-18**	0	0	-9	0	-9	0	0	0	**-27**	-9	-9	0	0
Disentis	RF_{obs}	0	5	30	35	40	40	75	55	45	30	10	0	75	65	50	35	20	20
	RF_{sim}	0	10	35	40	40	50	75	60	40	25	10	5	85	65	40	20	15	10
	Δ	0	5	5	5	0	10	0	5	-5	-5	0	5	10	0	-10	**-15**	-5	-10
Montana	RF_{obs}	0	3	7	10	10	24	90	83	72	59	45	31	83	72	59	45	34	24
	RF_{sim}	0	10	10	17	23	30	83	63	57	43	43	37	80	60	57	40	30	23
	Δ	0	7	3	6	**13**	6	-6	**-19**	**-16**	**-15**	-1	6	-3	**-12**	-2	-5	-4	-1
Davos	RF_{obs}	0	0	0	0	4	10	100	100	96	80	62	36	100	96	80	60	48	26
	RF_{sim}	0	0	0	0	2	8	100	100	92	76	55	43	100	92	73	55	39	31
	Δ	0	0	0	0	-2	-2	0	0	-4	-4	-7	7	0	-4	-7	-5	-9	5
Weissfluhjoch	RF_{obs}	0	0	0	0	0	0	100	100	100	100	100	100	100	100	100	100	100	100
	RF_{sim}	0	0	0	0	0	0	100	100	100	100	100	100	100	100	100	100	90	80
	Δ	0	0	0	0	0	0	0	0	0	0	0	0	0	0	0	0	-10	**-20**

RF_{obs}, RF_{sim}: measured and simulated relative frequencies in the validation period, respectively; Δ: RF_{sim} minus RF_{obs}; h: snow depth threshold (in cm); $N_d(S \geq h)$: number of days within a given subperiod (P_i) of the year at which snow depth (S) exceeds h; P_2, P_3: subperiods of the year considered. All data are given in % and were computed using varying numbers of winters depending on the location (see Section 2.8). Deviations larger than 10% are shown in bold.

A quantitative assessment of the model's performance is given in Table 4, which compiles the validation results for $N_d(S \geq h)$. The correlation coefficients (r) between the observed and simulated N_d time series were generally highly significant. The mean (Δ) and mean relative (Δ%) errors were typically less than 3 d and 10%, respectively. Some larger negative biases were however obtained for Montana and Weissfluhjoch for the subperiods P_1 and P_2.

Table 5 shows the validation results for selected RF statistics. In 80 of the 3 x 6 x 5 = 90 conducted comparisons the differences between the observed and simulated statistics were below 10%. Errors larger than 10% occurred in 9 out of 52 cases where the observed RF was between 5% and 95%. The largest deviations were obtained for Engelberg and Montana, and for Weissfluhjoch in subperiod P_3. The simulations generally tended to overestimate the RFs of the "bad years" for skiing ($N_d < 40$) and to underestimate the RFs of the "good years".

3.2 Climate Change Scenarios from Spatial Downscaling

Fig. 5 shows the results obtained from the spatial downscaling procedure for selected climate parameters and the two GCM simulations. The ECHAM scenario (upper panels) specified a slightly warmer and drier wintertime climate as compared to the 1931-1980 conditions, whereas the CCC scenario (bottom panels) suggested a shift towards substantially warmer and wetter winters. Both scenarios specified a decrease for the within-month standard deviation of wintertime daily mean T. This decrease was more pronounced under the CCC scenario. Wintertime Pprob was found to systematically decrease in the ECHAM scenario, but it showed small or no changes in the CCC scenario.

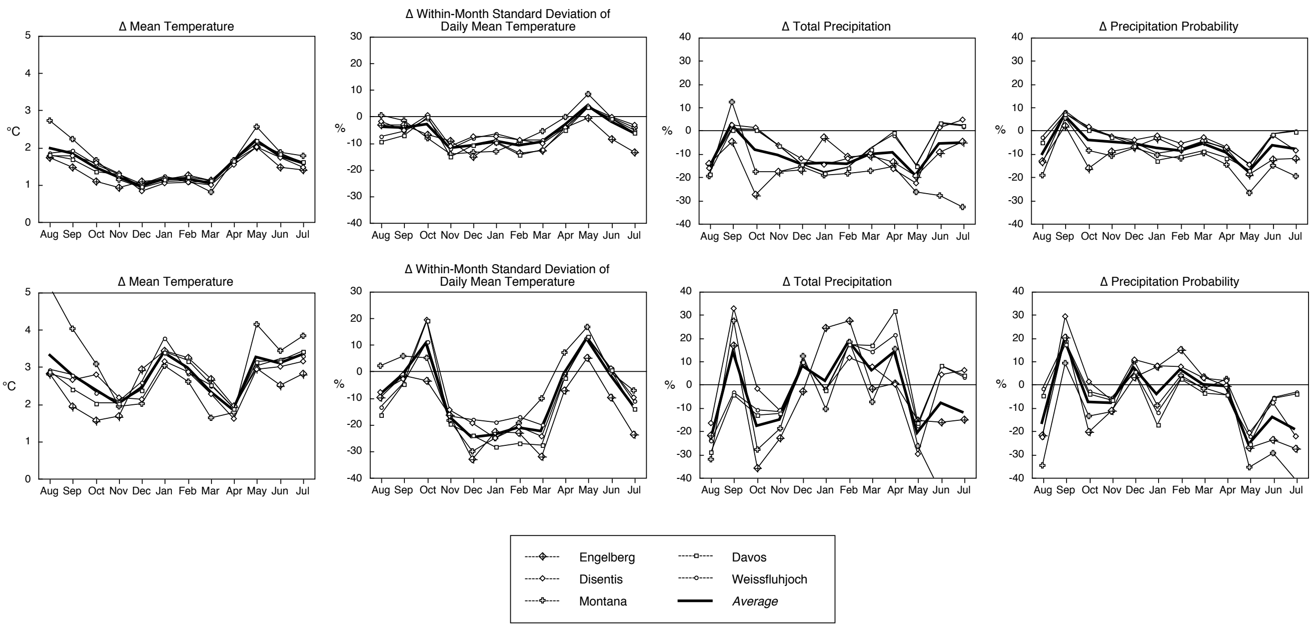

Figure 5: Changes (Δ) in selected climatic parameters according to the ECHAM (top) and CCC (bottom) climatic scenarios. All changes are given relative to the 1931-1980 baseline. See also Table 6.

Table 6: Average climatic changes for the winter half-year (November-April) according to the ECHAM and CCC climatic scenarios

Scenario / Location	ΔTmean (°C)	ΔTmin (°C)	ΔTmax (°C)	ΔSDTm (%)	ΔSDTn (%)	ΔSDTx (%)	ΔPrecip (%)	ΔPprob (%)
ECHAM								
Engelberg	1.19	1.36	1.03	-10.7	-10.7	-10.7	-12.5	-6.9
Disentis	1.13	0.96	1.12	-8.2	-8.4	-9.1	-12.2	-4.4
Montana	1.12	1.12	1.21	-9.3	-9.9	-6.9	-17.6	-11.2
Davos	1.22	1.22	1.29	-11.3	-10.0	-11.0	-10.8	-9.1
Weissfluhjoch	1.23	1.24	1.07	-8.2	-6.5	-10.5	-10.8	-6.6
Average	*1.18*	*1.18*	*1.15*	*-9.5*	*-9.1*	*-9.6*	*-12.8*	*-7.6*
CCC								
Engelberg	2.63	2.80	2.46	-22.4	-21.1	-21.1	4.2	2.9
Disentis	2.35	2.13	2.19	-17.7	-17.1	-18.7	2.7	4.0
Montana	2.14	2.25	2.15	-16.0	-17.2	-10.9	1.5	-0.9
Davos	2.55	2.59	2.52	-21.6	-18.1	-20.9	10.1	-4.0
Weissfluhjoch	2.60	2.57	2.18	-15.4	-10.1	-15.3	8.2	-2.5
Average	*2.45*	*2.47*	*2.30*	*-18.6*	*-16.7*	*-17.4*	*5.3*	*-0.1*

Shown are changes relative to the 1931-1980 baseline. ΔTmean, ΔTmin, ΔTmax: changes in the monthly mean, mean daily minimum, and mean daily maximum temperature; ΔSDTm, ΔSDTn, ΔSDTx: changes in the within-month standard deviations of the daily mean, daily minimum and daily maximum temperatures; ΔPrecip: change in monthly total precipitation; ΔPprob: change in monthly precipitation probability. See also Figure 5.

The winter half-year average changes that were obtained from spatial downscaling for the 8 monthly input variables of relevance to the snow cover simulations are summarized in Table 6. In the ECHAM scenario the temperature minima showed at three locations smaller changes as compared to the maxima, whereas in the CCC scenario the minima showed similar or larger changes than the maxima. The within-month standard deviations of the three T variables generally showed changes of similar magnitude for a given location and scenario.

3.3 Climatic Sensitivity of Snow Depth Statistics

The simulated responses of the long-term mean seasonal cycles of S to the various climate change scenarios are shown in Fig. 6. Several observations can be made:

First, the simulations specified a general decrease in S. An exception occurred for the scenarios T2Pp, T4Pp and CCC at Weissfluhjoch, where only small changes or even slight increases were obtained for the period from October through March or April. Second, the T2 scenarios always yielded smaller changes than their T4 counterparts that assumed the same changes in P. Third, for a given change in T the Pm scenarios yielded generally larger decreases than the Pp scenarios. The effect of the Pm scenarios was more pronounced under the T2 scenarios as compared to the T4 scenarios, and it increased with elevation. Fourth, the relative response to the two GCM-downscaled scenarios also showed a clear elevation dependency: The CCC scenario yielded a stronger signal than the ECHAM scenario at the three lowest sites, but the differences decreased with elevation and at the high-elevation site Weissfluhjoch they were even reversed. Finally, from Fig. 6 it can be seen that the largest decreases in long-term mean snow cover were typically obtained in spring, such that in most cases the date of the maximum snow depth was shifted towards earlier in the winter season.

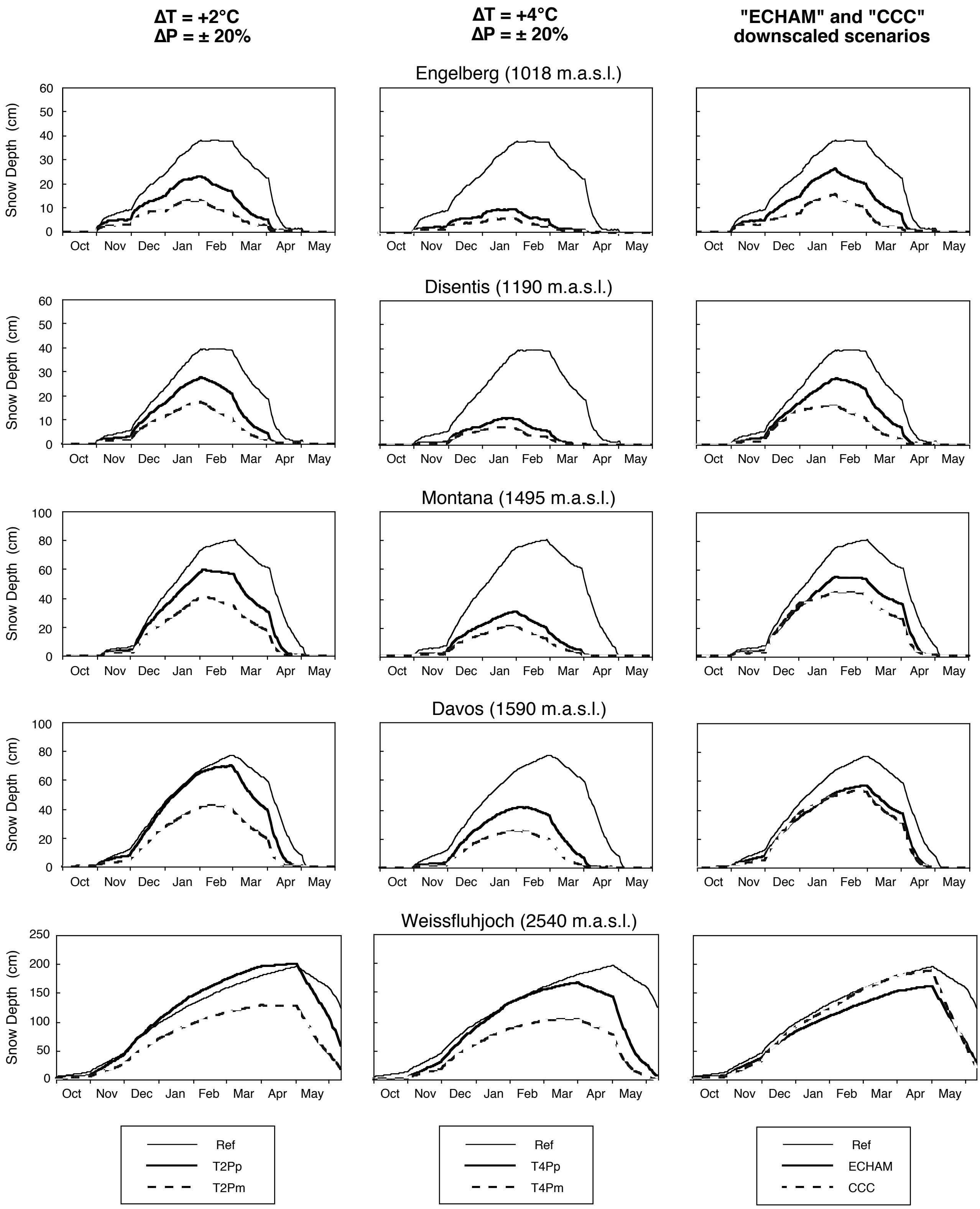

Figure 6: Effect of different climate change scenarios on simulated long-term mean daily snow depths at the five case study sites. Ref: simulated snow depths for the reference (present-day) climate, winters 1981/82-1994/95 (cf. Figure 3); T2Pp, T2Pm, T4Pp, T4Pm, ECHAM, CCC: simulated snow depths under the respective scenarios of climatic change.

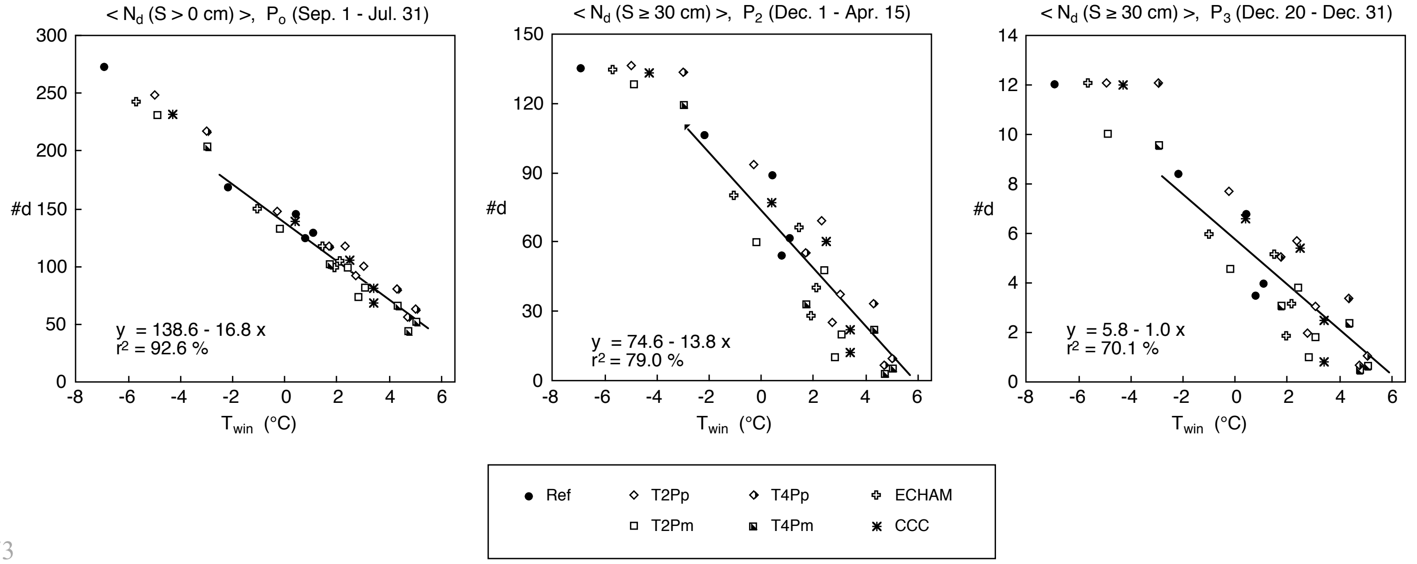

Figure 7: Simulated long-term mean numbers of days ($\langle N_d(\ldots)\rangle$) at which snow depth (S) exceeds a given threshold (0 or 30 cm) within selected subperiods (P_o, P_2 or P_3) of the year as a function of winter half-year (November-April) long-term mean temperature (T_{win}). Ref: simulated values for the reference (present-day) climate, winters 1981/82-1994/95; T2Pp, T2Pm, T4Pp, T4Pm, ECHAM, CCC: simulated values under the respective scenarios of climatic change. See also Table 7.

Table 7: Simulated temperature sensitivities for the long-term mean numbers of days at which snow depth exceeds a given threshold within selected subperiods of the year

	P_o (Oct. 1 - May 31)				P_2 (Dec. 1 - Apr. 15)				P_3 (Dec. 20 - Dec. 31)			
h	$\langle \overline{N}_d \rangle$	AS	RS	r^2	$\langle \overline{N}_d \rangle$	AS	RS	r^2	$\langle \overline{N}_d \rangle$	AS	RS	r^2
(cm)	(#d)	(#d/°C)	(%/°C)	(%)	(#d)	(#d/°C)	(%/°C)	(%)	(#d)	(#d/°C)	(%/°C)	(%)
0	101.0	-16.8	-16.6	92.6	88.4	-12.9	-14.6	88.2	9.0	-1.0	-11.6	77.0
10	72.2	-16.6	-22.9	87.0	67.6	-14.9	-22.0	85.3	6.6	-1.3	-20.1	78.8
20	56.3	-15.7	-27.8	83.1	54.2	-14.8	-27.3	82.4	4.8	-1.2	-25.0	74.5
30	44.6	-14.3	-32.0	79.3	43.6	-13.8	-31.7	79.0	3.6	-1.0	-28.4	70.1
40	35.4	-12.6	-35.6	75.2	34.9	-12.3	-35.3	75.1	2.6	-0.8	-30.4	65.8
50	28.1	-10.9	-38.8	70.6	27.9	-10.7	-38.6	70.6	1.9	-0.6	-31.5	59.1

P_o, P_2, P_3: subperiods of the year considered; h: snow depth threshold; $\langle \overline{N}_d \rangle$: average for all sites and scenarios used to compute sensitivities of the long-term mean number of days ($\langle N_d \rangle$) within a given subperiod (P_i) of the year at which snow depth exceeds h; AS: absolute sensitivity, $\partial\langle N_d\rangle/\partial T_{win}$, where T_{win} = winter half-year (November-April) long-term mean temperature; RS: relative sensitivity, $(\partial\langle N_d\rangle/\partial T_{win})/\overline{N}_d$; r^2: percentage of variance explained by the linear regression used to estimate $\partial\langle N_d\rangle/\partial T_{win}$. Results were based on simulated snow depths at the sites Engelberg, Disentis, Montana and Davos under present-day and changed climatic conditions according to the scenarios T2Pp, T2Pm, T4Pp, T4Pm, ECHAM and CCC. The average T_{win} for the four sites and all scenarios was 2.2 °C. All sensitivities apply to the temperature range -2.2 °C to +5.1 °C. See also Figure 7.

Fig. 7 shows the simulated long-term means ($\langle N_d \rangle$) of selected $N_d(S \geq h)$ statistics as a function of T_{win}. The $\langle N_d \rangle$ for the days with snow lying on the ground (top left panel) was found to decrease by ~17 d per °C change in T_{win}. In most cases the $\langle N_d \rangle$ were found to remain close to their respective maximum values for T_{win} below ca. -2 °C, but above this threshold they showed a more or less linear decrease with increasing T_{win}.

The sensitivities $\partial\langle N_d\rangle/\partial T_{win}$ for various subperiods of the year and snow depth thresholds are summarized in Table 7. The sensitivities were estimated using all data points that fell between the two extreme states $\langle N_d\rangle$ = maximum number of days (Table 3) and $\langle N_d\rangle = 0$. It can be seen that the AS tended to decrease with increasing snow depth h, whereas for the RS was found the opposite result. The robustness of the sensitivity estimates (as measured by the r^2 of the regressions) was also found to decrease with increasing h and with decreasing length of the subperiod of the year considered.

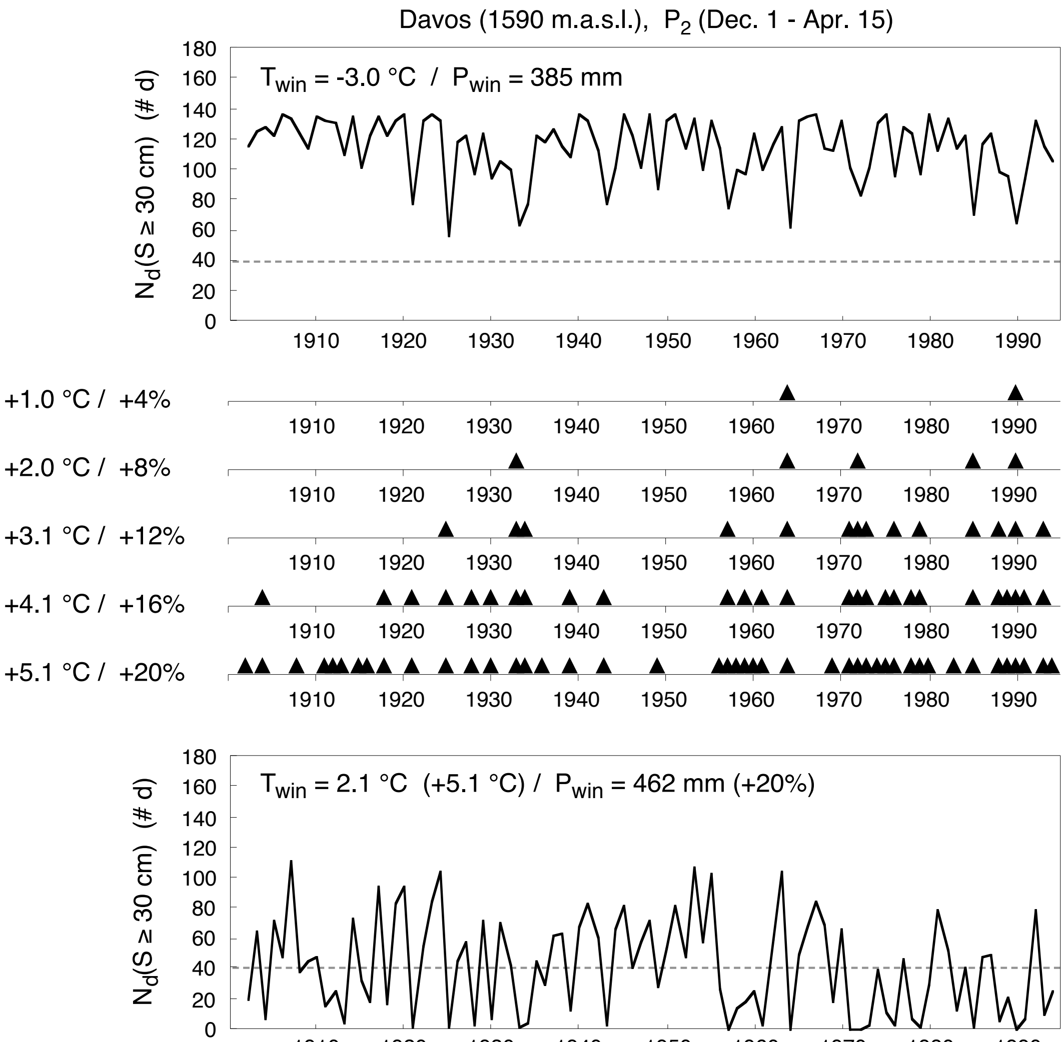

Figure 8: Simulated numbers of days at which snow depth exceeds 30 cm in the subperiod P_2 (Nov. 1 - Apr. 30) at Davos under present conditions (top panel) and under the CCC-TR(s=2.0) scenario (bottom panel). The panels inbetween show the years with simulated number of days < 40 d (event signified by ▲) for the scenarios CCC-TR(s=0.4) to CCC-TR(s=2.0), with s varying in steps of 0.4 ("s" denotes the factor used to scale the original CCC scenario, see Section 2.8). T_{win}, P_{win}: winter half-year (November-April) long-term mean temperature and precipitation, respectively; xx °C / yy %: assumed changes in T_{win} / P_{win} under the respective scenario.

Fig. 8 shows the simulated $N_d(S \geq 30\text{ cm})$ time series for Davos in subperiod P_2 under present (top panel) and CCC-TR(2.0) (bottom panel) scenario conditions. The panels in between indicate the occurrence of "bad" years for skiing for a subset of the CCC-TR scenarios. It can be seen that the "bad" years' frequency increased over-proportionally with increasing T_{win}.

From the comparison of the top and bottom panels in Fig. 8 it can further be discerned that the assumed changes in climate lead to distinct shifts in the shape of the snow variables' statistical distribution. For instance, the standard deviation of the simulated N_d was found to increase from 20.4 d under present conditions (top panel) to 31.7 d under the CCC-TR(2.0) scenario (bottom panel, +56%), and the skewness of the time series changed from -0.97 (top panel) to +0.33 (bottom panel).

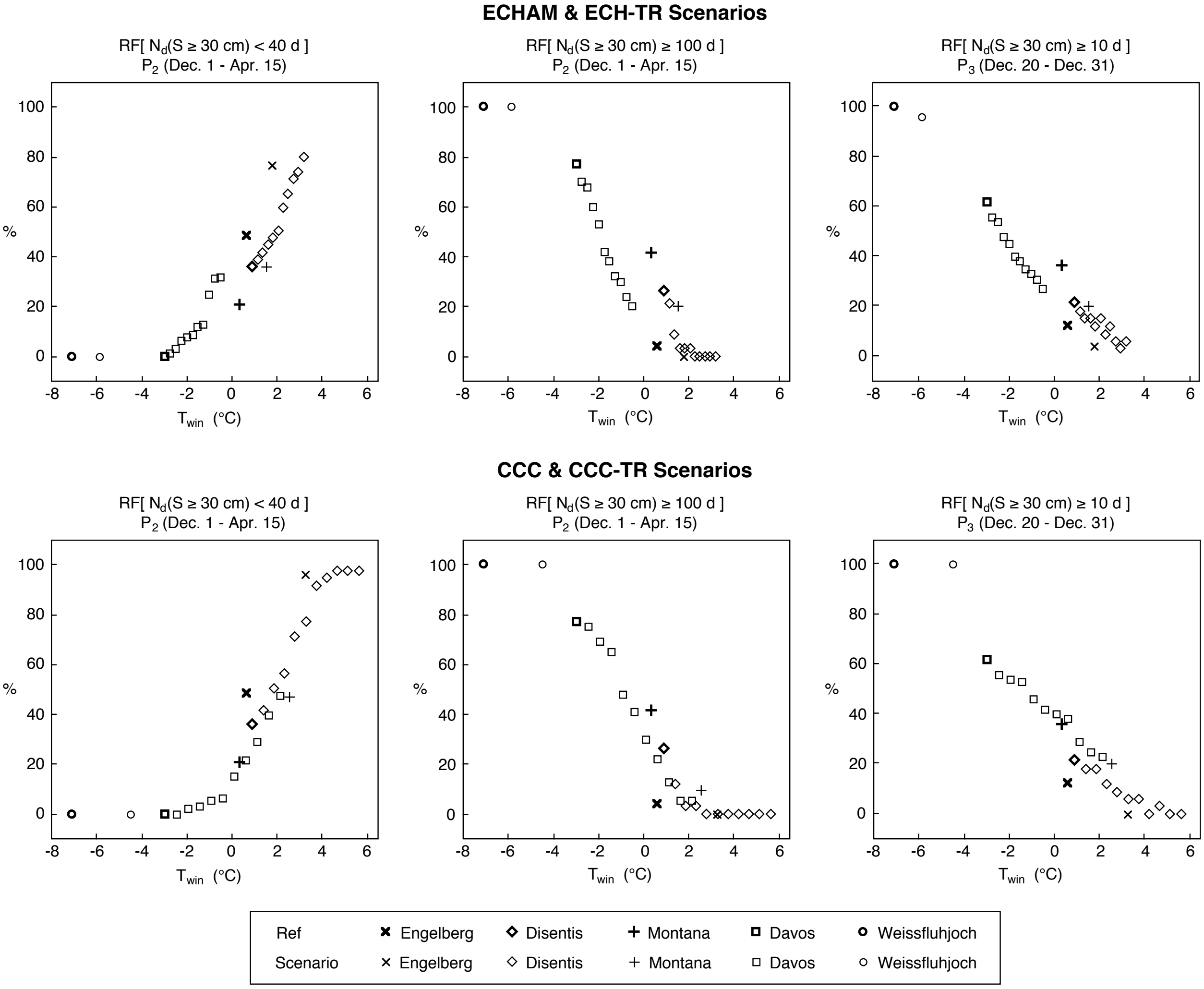

Figure 9: Simulated relative frequencies (RF) of years with selected snow cover characteristics as a function of winter half-year (November-April) long-term mean temperature (T_{win}). $N_d(S \geq h)$: number of days at which snow depth exceeds h; P_2, P_3: subperiods of the year considered; Ref: simulated relative frequencies for the reference (present-day) climate; ECHAM, ECH-TR, CCC, CCC-TR: simulated relative frequencies under the respective scenarios of climatic change. The simulations considered a varying number ($\geq$ 24) of winters, depending on the location (see Section 2.7). See also Table 8.

Table 8: Simulated temperature sensitivities for the relative frequencies of years with selected snow cover characteristics

	RF[$N_d(S \geq h) < 40$ d] P_2 (Dec. 1 - Apr. 15)				RF[$N_d(S \geq h) \geq 100$ d] P_2 (Dec. 1 - Apr. 15)				RF[$N_d(S \geq h) \geq 10$ d] P_3 (Dec. 20 - Dec. 31)			
h	$\overline{RF}$	Range T_{win}	AS	r^2	$\overline{RF}$	Range T_{win}	AS	r^2	$\overline{RF}$	Range T_{win}	AS	r^2
(cm)	(%)	(°C)	(%/°C)	(%)	(%)	(°C)	(%/°C)	(%)	(%)	(°C)	(%/°C)	(%)
0	20.2	+1.6..+5.7	14.3	83.3	54.0	-1.0..+3.8	-18.8	83.5	63.1	-0.8..+5.7	-10.1	54.8
10	31.9	-0.8..+5.2	14.7	82.7	47.0	-2.2..+2.9	-15.7	86.5	54.0	-3.0..+5.7	-11.1	81.8
20	39.9	-1.5..+4.8	13.6	79.3	46.8	-3.0..+2.6	-14.3	84.5	37.9	-3.0..+5.2	-9.9	82.5
30	42.2	-2.2..+4.3	13.1	82.4	36.6	-3.0..+2.6	-12.5	81.4	28.2	-3.0..+3.8	-8.0	86.3
40	45.8	-2.7..+3.8	13.3	85.5	29.1	-3.0..+2.6	-9.5	76.6	25.4	-6.6..+2.6	-6.4	88.6
50	52.2	-3.0..+3.3	12.7	85.9	26.3	-6.6..+1.6	-8.7	84.7	24.2	-7.8..+2.6	-7.5	83.4

RF: relative frequency; $N_d(S \geq h)$: number of days within a given subperiod (P_i) of the year at which snow depth (S) exceeds h; P_2, P_3: subperiods of the year considered; $\overline{RF}$: average RF for all sites and scenarios used to compute a sensitivity; T_{win}: winter half-year (November-April) long-term mean temperature; AS: absolute sensitivity $\partial RF/\partial T_{win}$; r^2: percentage of variance explained by the linear regression used to estimate $\partial RF/\partial T_{win}$. Results were based on simulated snow depths under present-day and changed climatic conditions according to the scenarios ECHAM and CCC (all five case study sites), plus scenarios ECH-TR and CCC-TR (sites Disentis and Davos only). The simulations considered a varying number ($\geq$ 24) of winters, depending on the location (see Section 2.7). The sensitivities were determined using simulation results from all sites and scenarios for which T_{win} fell within the specified range. See also Figure 9.

Generally, changes in the interannual variability of the various N_d time series were found to depend on the threshold h, the subperiod of the year, and T_{win} (results not shown). On average over all locations and scenarios, the variability was found to increase with increasing T_{win} up to a certain critical value, T_{crit}, and then to decrease again above this value. T_{crit} tended to decrease with increasing h and with increasing length of the subperiod used to compute the snow depth statistics. For instance, for h = 0 cm and P_o was T_{crit} = 2.9 °C, and for P_3 was T_{crit} = 4.2 °C; for h = 30 cm T_{crit} ranged between -0.2 °C and +0.9 °C; and for h = 50 cm it was between -1.2 °C and -0.6 °C.

Fig. 9 shows selected RF statistics as a function of T_{win}. The RFs of the simulated "bad" years for skiing (left panels) were generally found to increase, and the RFs of the "good years" (middle and right panels) to decrease with rising T_{win}. The average rates of change per degree change in T_{win} depended somewhat on the choice of the scenario and statistic. For instance the RFs of the "good years" were found to decrease more strongly under the ECHAM and ECH-TR scenarios (top panels in Fig. 8) as compared to the CCC and CCC-TR scenarios (bottom panels).

Table 8 gives a summary of the simulated average sensitivities $\partial RF/\partial T_{win}$. They were estimated using all RF values in the range 5% to 95%. The sensitivities of the "bad" years for skiing (Table 8, left) were found to slightly decrease with increasing snow depth threshold h. An even stronger decrease of sensitivity with h was obtained for the "good" years (Table 8, middle and right). The r^2 of the regressions were generally above 75%; the only exception occurred for h = 0 cm and subperiod P_3. In this case only a limited sample of RF values above 5% was available to estimate the $\partial RF/\partial T_{win}$ (not shown).

3.4 Comparison with Earlier Swiss Studies

BULTOT et al. (1992) used the daily time step, lumped-parameter conceptual model IRMB to study changes in the hydrology of the Murg basin in northern Switzerland (212 km^2, elevation range 390-1035 m, average 580 m). They assumed changes in T_{win} by +3.2 °C and in winter total precipitation (P_{win}) by +11%, and obtained for long-term mean $N_d(S > 0$ cm) in subperiod P_o AS = -18.2 d/°C and RS = -23 %/°C (their Table 2). This compares with AS = -16.6 d/°C and RS = -16.6 %/°C reported in Table 7.

BULTOT et al. (1994) applied the IRMB model also to the Broye catchment in western Switzerland (392 km^2, 441-1514 m, average 710 m). They considered a seasonally uniform warming by 1 °C and 2 °C, respectively, with no changes in precipitation, plus the same climate change scenario as BULTOT et al. (1992). Their simulations yielded for long-term mean $N_d(S > 0$ cm) in subperiod P_o and on average over the two elevation zones 900-1200 m and 1200-1500 m AS = -22.8 d/°C, RS = -18 %/°C (their Table III). For our three lowest locations (1018-1495 m) we obtained AS = -18.4 d/°C and RS = -21 %/°C (not shown). For long-term mean $N_d(S \geq 30$ cm) in the subperiod December to April and the elevation zone 1200-1500 m their work yielded AS = -19.3 d/°C, RS = -21%/°C (their Table IV). Our result for the same elevation range (i.e., locations Disentis and Montana) and the subperiod P_2 was AS = -15.6 d/°C, RS = -38 %/°C.

SCHULLA (1997) investigated possible changes in the hydrology of the Thur catchment in northern Switzerland (1700 km^2, 356-2504 m, average 769 m) using the WaSiM-ETH distributed parameter model. He used three climate change scenarios that assumed changes in Twin by +1.2 °C, +2.3 °C and +2.9 °C, and in P_{win} by +11%, +9% and +16%, respectively. His simulations (his Fig. 4.13) give for long-term mean $N_d(S \geq 10$ cm) in subperiod P_o and the elevation range 1100-1700 m AS = -25.8 d/°C and RS = -29 %/°C. Our corresponding estimates (Table 6) were AS = -16.6 d/°C, RS = -23 %/°C. For long-term mean $N_d(S \geq 30$ cm) he obtained -21.8 d/°C (-42 %/°C) whereas our simulations (Table 7) yielded -14.3 d/°C (-32 %/°C).

STADLER et al. (1998) employed the SOIL one-dimensional coupled mass and heat transfer model for point hydrological simulations at the sites Engelberg and Davos. They used two incremental scenarios that assumed a seasonally uniform temperature increase by 1.5 °C and 3 °C, respectively, and no changes in precipitation, plus two scenarios that specified site-specific changes for T_{win} and P_{win} (Engelberg: +1.3 °C, -11% and +2.2 °C, -11%; Davos: +1.0 °C, -3%, +1.8 °C, +6%). For long-term mean annual mean snow depth at Engelberg they obtained AS = -1.8 cm/°C, RS = -47 %/°C and for Davos AS = -4.3 cm/°C, RS = -37 %/°C (their Tables 4.1 and 4.2). The corresponding average values from our simulations were for Engelberg -3.1 cm/°C (-46 %/°C) and for Davos -4.6 cm/°C (-40 %/°C) (not shown, cf. Fig. 6).

EHRLER (1998; see also SEIDEL et al. 1998) used the SRM semi-distributed (elevation zones) conceptual model to simulate possible changes in snow accumulation and runoff for the Upper Rhine basin in central/eastern Switzerland (3250 km^2, 560-3614 m, average 2000 m; our sites Disentis, Davos and Weissfluhjoch are located within this basin). He employed 15 climatic scenarios which specified seasonally uniform changes in T_{win} between 0 °C and 3.8 °C and in P_{win} between 0% and +20%. For the areal mean, long-term mean water equivalent of the snow cover in the elevation range 1100-2600 m his study gave AS = -6.0 cm/°C, RS = -16%/°C (his Table 29). Assuming an average snow density of 0.4 to 0.5 kg/m^3 this AS value translates to a sensitivity for the annual mean snow depth of -12 to -15 cm/°C. The corresponding sensitivities from our 4 highest sites (1190-2540 m) were AS = -18.2 cm/°C, RS = -13%/°C (cf. Fig. 6).

BENISTON et al. (2003a) used meteorological and snow depth measurements from 18 Swiss stations in the elevation range 317-2500 m to derive an empirical response surface to predict long-term mean $N_d(S > 0$ cm) in subperiod P_o as a function of December to February mean temperature and precipitation. They considered a 2 °C warming and they state for the sites Arosa at 1847 m and Säntis at 2500 m AS = -25 d/°C (both sites), RS = -22 %/°C (Arosa) and -9 %/°C (Säntis). Our results for Davos (1590 m) and Weissfluhjoch (2540 m) were AS = -14.6 d/°C and -15 d/°C and RS = -11 %/°C and -6.4 %/°C, respectively (cf. Fig. 7, left).

BENISTON et al. (2003b) analyzed the same empirical data set, and for $N_d(S > 0$ cm) and subperiod P_o they suggested for all elevations an AS range between -15 d/°C and -20 d/°C. Our corresponding estimate was AS = -16.6 d/°C (Table 7).

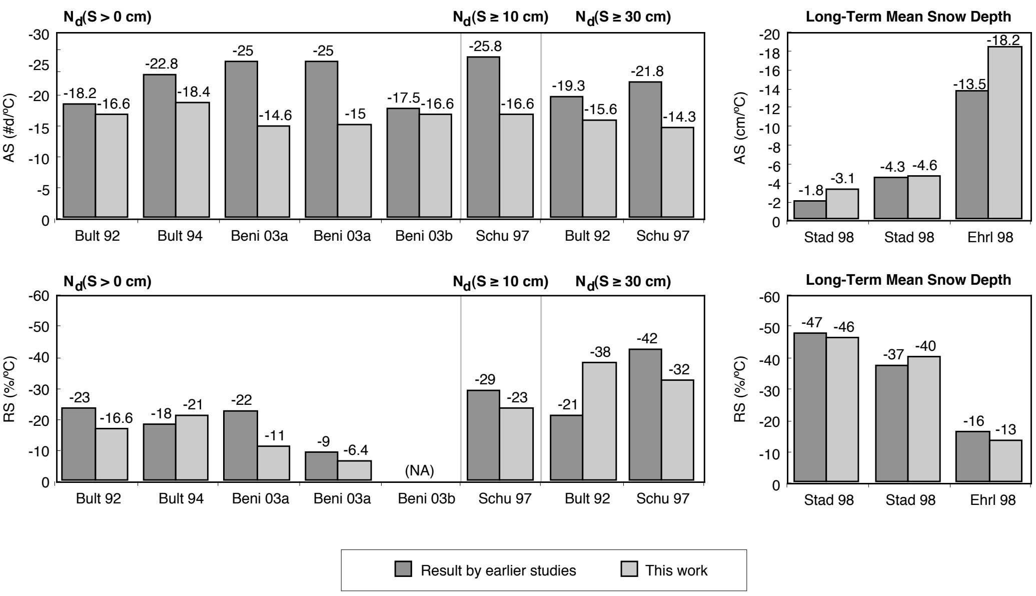

Figure 10: Comparison of estimated sensitivities of snow cover statistics with the results from earlier Swiss studies. Top: Absolute sensitivities (AS); bottom: Relative sensitivities (RS). $N_d(S \geq h)$: long-term mean number of days at which snow depth exceeds h. All statistics refer to subperiod P_o, except for the rightmost N_d statistic which refers to subperiod P_2. NA: data not available. Bult 92: BULTOT et al. (1992); Bult 94: BULTOT et al. (1994); Beni 03a: BENISTON et al. (2003a); Beni 03b: BENISTON et al. (2003b); Schu 97: SCHULLA (1997); Stad 98: STADLER et al. (1998); Ehrl 98: EHRLER (1998). Note, the earlier studies considered in most cases other regions, locations, climatic baselines and/or climate scenarios than the ones used in this study. Comparison was done using the most similar results available from the present work. For details see text.

Finally, WIELKE et al. (2004) investigated the sensitivity of snow cover at 59 Swiss stations to interannual variations in European winter mean temperature (T_{winE}). They considered $N_d(S \geq 5$ cm) for winter (December to February) and spring (March to May), and they defined sensitivity by the maximum slope of a fitted logistic curve $N_d = f(T_{winE})$ (cf. Figs. 7 and 9). They found for winter AS = -27.3 d/°C and for spring AS = -35.9 d/°C.

The results of our comparisons are summarized in Fig. 10. The study by WIELKE et al. (2004) was not included in this figure because of the very different definition of sensitivity in this work (use of European temperature T_{winE}) as compared to all other studies (use of regional or local temperatures). This issue is discussed in more detail in Section 4.1.2.

From Fig. 10 can be seen that our sensitivity estimates were generally lower than those obtained in earlier studies. The found differences were somewhat smaller for long-term mean snow depth (Fig. 10, right) as compared to the N_d statistics (left) and for the RS (bottom) as compared to the AS (top) statistics.

3.5 Comparison with Other Regions

Various studies have addressed the sensitivity of snow cover in other regions. Below we discuss a selection of quantitative results known to us. We focus on the AS of the long-term mean number of days with snow lying on the ground, $N_d(S > 0$ cm) during subperiod P_o (here simply abbreviated as N_d) since this was the most frequently reported statistic.

For Austria KOCH & RUDEL (1990) estimated based on a statistical analysis of measured temperatures and snow cover data AS = 25 d/°C. HANTEL et al. (2000) applied a much more sophisticated analysis technique to an extensive empirical data base from the same region and obtained for winter (for spring) AS = 31 d/°C (42 d/°C).

For the French Alps MARTIN et al. (1994) investigated the sensitivity of the coupled SAFRAN/CROCUS meteorological-analysis and multi-layer snow models to changed temperature and radiation conditions as derived from a "double CO_2" GCM experiment. Their results suggested for N_d at 1500 m (at 3000 m) AS = 17-22 d/°C (11-17 d/°C).

MARTIN et al. (1997) combined the same modelling system with a spatial downscaling procedure and considered climatic changes as simulated by two further GCMs. For areal mean N_d in the Mont-Blanc region in the north-eastern part of the French Alps they reported (their Fig. 8 and Table 4) at 1500 m AS = -29 d/°C (RS = -19.4 %/°C). For the Mercantour massif in the south-eastern part of the French Alps they obtained for the same elevation AS = -28.3 d/°C (RS = -45.4 %/°C).

The sensitivities of the Estonian and the Scottish snow cover have been assessed based on the analysis of observed snow cover-temperature covariations. JAAGUS (1997) found for the West-Estonian archipelago ($T_{win} < -1$ °C) AS = -11 to -12 d/°C, and for the cooler ($T_{win} = -3$ to -5 °C) inland and eastern parts of Estonia AS = -7 to -10 d/°C. HARRISON et al. (2001) reported for Scotland an average value of AS = -9 d/°C.

Finally, the sensitivity of south-east Australian snow cover has been studied by WHETTON et al. (1996). On average over 8 locations in the elevation range 1564 m to 2228 m their results (their Table III) suggest for temperature changes of up to 2 °C and precipitation changes between -10% and +20% AS = -32.1 d/°C (RS: -38 %/°C) (Note, these numbers do not consider their "year 2070 worst-case" scenario because under this assumption they obtained for most sites no snow cover at all). As was the case in the present study their sensitivities tended to decrease with elevation. However, quite differently from our results (Fig. 6), they concluded that under a general warming precipitation changes up to 20% would have only a small impact on the snow cover duration.

4. Discussion

4.1 Climatic Sensitivity of the Swiss Snow Cover

Our results (Figs. 6 to 8, Tables 7 to 9) indicate that a mean temperature increase in the order of 2 °C to 4 °C would lead to a general decrease in the average duration and depth of Swiss snow cover, at least up to elevations of ~2500 m. This decrease would show marked regional and seasonal variations, and it would be significantly modulated by possible changes in precipitation (Figs. 6, 7 and 9).

The largest sensitivities to a warming (Figs. 6 and 9) were generally obtained at the three lower-elevation sites. This can be explained by the fact that at these sites the present-day winter mean temperature is close to, or only slightly above the freezing point (cf. Table 1).

The found high sensitivity at lower elevations is consistent with the results from several observational studies: Based on an analysis of data from 12 Swiss locations (elevation range 276-2540 m) for the period 1980-1994 Beniston (1997) found a strong increase in relative variability (defined as the standard deviation divided by the mean) of $N_d(S \geq h)$ with decreasing elevation and increasing h; he thus concluded that snow cover at sites below 1500 m is increasingly sensitive to the occurrence of warm winters. Beniston et al. (2003b) also studied possible changes in long-term mean Swiss total snow volume due to a wintertime warming by +2 and +4 °C using data from 18 Swiss stations and they also found a decreasing sensitivity with elevation. Laternser & Schneebeli (2003) analyzed snow cover variations at 140 Swiss stations for the period 1931-1999. For the particularly warm, last two decades of the 20th century they detected a general decrease in winter mean snow depths, which increased with decreasing elevation. A similar result was also reported by Scherrer et al. (2004). Finally, Wielke et al. (2004) estimated that the elevation of maximum sensitivity for the Swiss snow cover is 580 m in winter and 1370 m in spring.

Our results demonstrated a stronger sensitivity of the snow cover to a warming during spring as compared to early winter (Fig. 6). This finding suggests that the effects of a general temperature increase are dampened by the seasonal cooling at the beginning of the snow season, but that they are amplified by the seasonal warming at the end of the snow season.

The found seasonal variation in the snow cover's sensitivity is also in line with earlier studies: Föhn (1990) suggested that under a 3 °C temperature increase (and given no major changes in precipitation) the snow cover at an elevation of ~1500 m would build up later, at the first half of December, and that it would disappear already by the end of March. Our results for Montana and Davos (Fig. 6) are remarkably consistent with his assessment. Laternser & Schneebeli (2003) found in their analysis of long-term Swiss snow measurements a weak trend towards a later build up of snow cover at mid elevations (1000-1600 m) and a general trend towards earlier melting of the snow cover. This result is again supported by the empirical study of Wielke et al. (2004), who found smaller sensitivities for winter as opposed to spring.

The higher sensitivity during springtime has also been found in the modelling studies by Ehrler (1998) for the Upper Rhine basin; by Beniston et al. (2003b) for the site Säntis (2500 m), based on experiments with the GRENBLS surface energy balance model; and by Jasper et al. (2004), who applied the WaSiM-ETH model in the Thur and Ticino catchments to a range of climate change scenarios. The latter study reported a delay in the onset of the snow season by 1 to 3 weeks, and an earlier begin of snow-free conditions at 1000 m by 5 to 8 weeks, depending on scenario. They attributed the strong response during the melting period to the seasonal warming pattern in their scenarios. Our simulations using seasonally uniform changes in temperature (Fig. 6) suggest, however, that the main reason for this response is the amplification of the climate change signal by the seasonal warming during springtime.

Fig. 6 demonstrated that in our study region a decrease (an increase) in average precipitation would reinforce (counteract) the simulated negative effects of a warming on the snow cover (Fig. 6). This precipitation effect has also been noted by BENISTON et al. (2003a, 2003b), who found a smaller temperature sensitivity of Swiss snow volume for wetter-than-average winters as compared to dry winters.

Our results suggest that the compensating effect of a precipitation increase is smaller at lower elevations and during spring, as compared to higher elevations and during winter (Fig. 6). This appears plausible, since it can be expected that with decreasing average temperatures an increasing proportion of precipitation will fall as snow (cf. Eqs. 5, Table 2). Accordingly, at the warmer, low-elevation sites the precipitation increases that were specified in the "warm/wet" CCC-scenario (Fig. 5) did not help much to alleviate the stronger decay of the snow cover as compared to the "cool/dry" ECHAM scenario. However, at the mid-elevation site Davos both scenarios gave similar changes, and at the site Weissfluhjoch the wetter CCC scenario even yielded a smaller decrease as compared to the ECHAM scenario (Fig. 6, right).

This increasing importance of changes in precipitation with increasing elevation has also been reported by MARTIN et al. (1997) for the French Alps and by EHRLER (1998, pp. 90-91) for Switzerland. He found that for October through March (his definition of the winter season) the effects of a 2 °C temperature increase on the snow cover could be compensated by a 20% precipitation increase above an elevation of ca. 2100 m. For a 3 °C warming he suggested a compensation point between 2100 and 2400 m. Our findings agree quite well with his estimates (see Fig. 6, site Weissfluhjoch).

4.2 Quantitative Comparison of Sensitivities

In spite of the general qualitative agreement with the results from the earlier Swiss studies, the quantitative comparisons (Fig. 10) showed that our simulations gave generally lower sensitivity values than reported previously. We believe that several different factors have contributed to this result:

1. Sampling uncertainty: Most earlier *model-based* studies have considered only a limited number of years (ten or so). Given the large temporal variability of the Swiss snow cover (LATERNSER & SCHNEEBELI 2003; Figs. 4 and 8) it seems therefore possible that at least part of the deviations is a statistical artefact. However, this explanation might not hold when comparing with earlier *empirical* studies, since these have typically used larger data samples.

Particularly large deviations were obtained as compared to the empirical study by BENISTON et al. (2003a) (Fig. 10, top). However, to our understanding, the sensitivity estimates quoted in this study were extracted from a simple response surface graph, and this rough procedure would translate into a large estimation variance. We therefore believe that the found differences (Fig. 10) are not statistically significant. BENISTON et al. (2003b) reported later for $N_d(S > 0$ cm) a sensitivity range of -15 d/°C to -20 d/°C. This result appears to have been inferred from a more robust statistical analysis and it is in much better agreement with our average estimate of -16.6 d/°C.

2. Limited comparability of studies: The various studies considered different regions, climatic baseline periods, or climate scenarios. Moreover, they employed alternative definitions of the winter mean temperature, of the snow depth thresholds defining a day with snow lying on the ground, or of the seasonal time windows used to compute the snow cover statistics. Note also that in most earlier studies snow depth was derived from the total water equivalent of the snow cover by assuming a constant snow density (e.g., Bultot et al. 1994, Schulla 1997), whereas in this study snow depth was modelled explicitly. The highly non-linear equations used to describe the settling of the snow cover (Eqs. 7, 8) suggest the potential for major deviations between the two approaches.

The fact that Wielke et al. (2004) obtained much higher AS values (between -27 d/°C to -36 d/°C) as compared to all other Swiss studies (including this one, see Fig. 10) seems to have been caused by such methodical differences. The main reason probably lies in their use of European mean temperatures (T_{winE}, sector 5-25 °E and 42.5-52.5 °N) to define the sensitivity, whereas all other Swiss studies used regional or local T_{win} variables. Since all sensitivity estimates are based on regressing a snow cover statistic on a temperature variable (Eq. 10, Fig. 7), the sensitivities can be expected to scale in a first approximation inversely with the standard deviation (SD) of the temperature variable. For the analysis period 1961-1990 considered by Wielke et al. (2004) we found $SD(T_{winS})/SD(T_{winE}) = 1.32$, where T_{winS} stands for the Swiss areal mean winter temperature (analyses not shown). Hence, the use of T_{winE} probably yields higher sensitivities by ca. 30%. Even bigger differences in sensitivity can be expected to occur when local temperatures are used, which show even larger variabilities than T_{winE} and T_{winS} (not shown).

A further reason probably relates to the use of a 5 cm snow depth threshold (h) by Wielke et al. (2004). When considering subperiod P_2 (which is the most similar seasonal time window available from our study as compared to the winter definition used by Wielke et al. 2004) it can be seen from our Table 7 that both, AS as well as RS, tend to increase with increasing h (at least for h < 20 cm). Hence, alternative definitions of h could also contribute to the higher values obtained by Wielke et al. (2004) as compared to our study.

3. Model limitations: It is remarkable that our results differ quite strongly from those obtained from simulations with distributed (Schulla 1997, Jasper et al. 2004) or semi-distributed (Bultot et al. 1992, 1994; Ehrler 1998) models, whereas they agree quite well with those obtained from another site-specific simulation approach (Stadler et al. 1998; see Fig. 10). We therefore surmise that the (semi-)distributed models tend to systematically overestimate the true sensitivity of the *local* snow cover. We speculate that this is due to discretisation effects, and/or because these models were tuned to simulate hydrology and snow cover at a relatively coarse spatial resolution, e.g. for gridboxes of size 0.25 km^2 (Schulla 1997) or for different elevation zones (Bultot et al. 1992, 1994; Ehrler 1998).

4. Data Problems: Some of the found differences may also have been caused by errors in the used input data sets. One important error source is the underestimation of solid precipitation due to rain gauge undercatch (e.g. Sevruk 1985), a factor that has been treated differently in the various modelling studies. Another problem relates to possible inconsistencies in the weather data used to tune or drive the models. For instance, at our

site Weissfluhjoch meteorological and snow data were not measured at exactly the same locations, and this may have caused some systematic deviations in our simulations.

Our quantitative comparison with results from other world regions (Section 3.5) considered only a limited sample of studies. Nevertheless, the comparison clearly suggests that beyond the general response patterns found in this and earlier studies (e.g., maximum sensitivity in situations where long-term mean temperatures are close to the freezing point; compensation of a warming by possible increases in precipitation) the currently available quantitative estimates for the sensitivity of the snow cover show substantial variation across regions. The only apparent pattern appears to be a somewhat lower sensitivity with increasing latitude (Scotland, Estonia) as compared to the European Alpine region. Yet, it is again not clear in as far these differences are real, since the various methodical problems discussed above with regard to the Swiss studies apply equally to any comparisons between regions.

A better explanation of the found differences between studies would require a much more rigorous intercomparison of data sets, analysis procedures, and models. This was however beyond the scope of this work.

4.3 Critique of Method

The proposed method (Fig. 1) has two salient features: (i) it employs a modular, linear "end-to-end" approach that deals separately with the spatial and the temporal variability of regional climate, and (ii) it makes extensive use of empirical data.

Feature (i) has the advantage that the individual steps can be flexibly used, tested and improved independently from each other. For example, our procedure enabled us to study sensitivities based on arbitrary assumptions as well as on GCM-derived local climatic scenarios (Figs. 5 and 6). Alternative scenarios could easily have been introduced based on simulations with other GCMs, or regional climate models (RegCMs), or any combination of climate scenario construction approaches (MEARNS et al. 2001).

The use of empirical data (ii) helped to increase the realism of our simulations, albeit at the cost of introducing problems related to data availability, the robustness of the used statistical relationships, and their stationarity under a changing climate.

These problems are probably less acute with regard to the temporal downscaling procedure and the snow model, where it was demonstrated that 5 and 14 years of data for model tuning, respectively, enable accurate simulation of the snow cover's variability over a wide range of time scales (Fig. 4, Tables 4 and 5). Our snow cover simulations tended however to underestimate long-term mean daily snow depths (Fig. 3, Table 4). This probably relates to the fact that the used version (v2.5b) of the WeathGen software implements a step-like change in the expected values of the daily temperature variables between months. This resulted into anomalously warm temperatures, and hence reduced snow accumulation, in the second halves of the early winter months. Newer versions of the WeathGen software that employ a smoother representation of temperature variables' annual cycle would probably allow to further improve our results.

Several improvements seem also possible with regard to the spatial downscaling procedure, for instance by using additional large-scale predictor fields and/or by adopting a daily time step (e.g., BUISHAND et al. 2004). Note, however, that our overall method is less sensitive to shortcomings of the spatial downscaling step as compared to other approaches that make direct use of downscaled weather data (e.g., Martin et al. 1997). This is because we use spatial downscaling only in order to estimate changes in long-term mean climate (Fig. 5, Table 6; see also von Storch 1999), whereas the local high-frequency weather variations are simulated accurately by means of temporal downscaling. Nevertheless, the scenario changes obtained for poorly downscaled variables (such as the monthly standard deviations of daily temperatures, see Gyalistras et al. 1994) can not be trusted much. Sensitivity analyses to test the importance of possible changes in these variables could be easily carried out with our method.

Note that the temporal downscaling procedure greatly helped to improve the robustness of our sensitivity estimates. Firstly, it enabled us to accurately simulate local snow cover statistics based on a limited number of monthly weather inputs (Figs 3 and 4, Tables 4 and 5). Purely statistical approaches that attempt to predict snow cover statistics from monthly (e.g., Breiling & Charamza 1999) or seasonal (e.g., Scherrer et al. 2004) mean temperature and precipitation typically yield r^2 values below 50%. Our model chain gave clearly better results (Table 4). Secondly, by providing a large number of possible daily weather developments the temporal downscaling approach enabled a robust estimation of the expected values of daily (Figs 3 and 6) or annual (Fig. 4) snow cover variables conditional on monthly weather. And finally, thanks to its computational efficiency, it allowed us to easily carry out thousands of simulations in order to explore a wide range of possible changes in climate (Figs 6 to 9). This contrasts with earlier studies (see Section 3.4) that have typically explored but a limited number of changes in climate parameters and annual weather courses.

Our method compares favourably with similar model-based approaches: Whetton et al. (1996) have also used monthly weather data to drive a local snow model. However, different from our study their model employed but a monthly time step. They reported for $N_d(S > 0\ \text{cm})$ a root mean square error of 30 days. The corresponding value from our simulations was 11 days (average over the four lowest locations for period P_1; cf. Table 4). Scott et al. (2002, 2003) combined the LARS daily weather generator (Semenov et al. 1998) with a daily snow model. They found that this model did not simulate individual years very reliably (Scott et al. 2002, p.26). Moreover, their weather generator is known to systematically underestimate the interannual variability of monthly weather variables (Mavromatis & Hansen 2001). This systematic error is likely to further distort the long-term snow cover statistics obtained in their simulations. Therefore we believe that our method gives more accurate results.

A major disadvantage of our simulation approach is that it does not consider many relevant processes and feedbacks, such as radiation and slope-aspect effects, the redistribution of snow by wind, the lowering of the freezing level in narrow valleys during heavy precipitation events, regional atmospheric circulations, or the albedo-temperature feedback. A further limitation arises from the fact that each site is simulated independently, such that the resulting scenarios are spatially not consistent if one wishes to consider individual years across locations.

Some of these problems could be solved by using physically based point simulation models (e.g. Essery et al. 1999), spatially distributed models (see Section 3.4), or even regional climate models (e.g., Kleinn 2002, Leung et al. 2004). However, to our knowledge, the feasibility (parameters, weather inputs) and capability of these modelling approaches to accurately simulate the temporal variability of snow cover over longer time scales (Fig. 4, Table 4) has yet to be demonstrated.

5. Conclusions

This work shows that by combining a temporal downscaling procedure with a conceptual snow model it is possible to accurately simulate the seasonal to decadal-scale variability of local snow cover based on only eight monthly variables related to temperature and precipitation. The mean and the interannual variability of several Swiss snow cover indices of importance to the winter tourism industry is well reproduced (mean relative errors < 15%, r = 0.7 to 0.9). Model performance generally decreases the shorter the seasonal time window used to define a snow cover statistic.

The Swiss snow cover below 1600 m is primarily governed by temperature, but precipitation becomes increasingly important with elevation. Temperature sensitivity increases with decreasing elevation, it is larger during spring as compared to earlier in the snow season, and it shows substantial inter-site variations. At elevations above 2500 m an increase in winter mean precipitation by 20% could offset the effects of a 4 °C warming, at least for the time from October through March.

Different snow cover statistics show widely varying sensitivities. However, the sensitivities depend systematically on the choice of the snow depth threshold and seasonal time window. Climate change will strongly affect the higher-order moments (variance, skewness) of annual snow depth indices. Frequencies of years with specific snow cover characteristics (e.g., suitability of natural snow conditions for downhill skiing) can be expected to change non-linearly with a gradual change in climate.

The simulated snow cover responses appear physically plausible and are generally consistent with earlier observational and modelling studies for our study area. Our site-specific simulation approach gives somewhat lower sensitivities than have been reported earlier for the Swiss region. Quantitative comparisons between studies are however currently hampered by major methodical problems. Rigorous, systematic intercomparisons are needed in order to better understand the obtained variations in the sensitivity of local snow cover between different studies or regions.

On average over all scenarios and sites investigated the long-term mean number of days with snow lying on the ground between September 1st and July 31st was found to decrease by 17 d per °C change in the winter half-year (November-April) mean temperature. The number of days with snow depth exceeding 30 cm in the main skiing season (December 1st through April 15th) was found to decrease by on average 14 d/°C. The relative frequency of years with at least 100 days with snow depth exceeding the 30 cm threshold during the same period was found to decrease by on average 12.5%/°C.

The comparatively low input requirements of our method enable reliable long-term reconstructions of snow cover statistics from monthly weather data, they justify the use of parsimonious climatic scenarios, and they contribute to enhancing the robustness of future snow cover projections. Moreover, our method was shown to be more accurate than alternative methods proposed in earlier studies. Its adaptation to alternative needs by climate impact analysts, or other radiative forcing scenarios, climate models and regions appears straight-forward.

Acknowledgements.

Research of DG and MS was supported by the EU-project "Modelling of the Impact of Climate Extremes" (MICE, EVK20CT2001-0018). Particular thanks go to B. Abegg and R. Bürki for many inspiring discussions. The provision of snow and weather data by the Swiss Federal Institute for Snow and Avalanche Research Davos (SLF) and MeteoSwiss is greatfully acknowledged.

6. REFERENCES

Abegg, B., 1996: Klimaänderung und Tourismus: Klimafolgenforschung am Beispiel des Wintertourismus in den Schweizer Alpen (Climate change and tourism: climate impact research exemplified by winter tourism in the Swiss Alps). vdf, Hochschulverlag AG an der ETH Zürich, 222 pp.

Baumgartner, M. and A. Rango, 1995: A microcomputer-based alpine snow-cover analysis system (ASCAS). *Photogrammetric Engineering and Remote Sensing*, **61,** 1475-1486.

Beckmann, B.-R. and T. A. Buishand, 2002: Statistical downscaling relationships for precipitation in the Netherlands and North Germany. *International Journal of Climatology*, **22,** 15-32.

Beniston, M., 1997: Variations of snow depth and duration in the Swiss Alps over the last 50 years: links to changes in large-scale climatic forcings. *Climatic Change*, **36,** 281-300.

Beniston, M., F. Keller, and S. Goyette, 2003: Snow pack in the Swiss Alps under changing climatic conditions: an empirical approach for climate impacts studies. *Theoretical and Applied Climatology*, **74,** 19-31.

Beniston, M., F. Keller, B. Koffi, and S. Goyette, 2003: Estimates of snow accumulation and volume in the Swiss Alps under changing climatic conditions. *Theoretical and Applied Climatology*, **76,** 125-140.

Boer, G. J., N. A. McFarlane, and M. Lazare, 1992: Greenhouse gas-induced climate change simulated with the CCC second-generation general circulation model. *Journal of Climate*, **5,** 1045-1077.

Braun, L. N. and C. B. Renner, 1992: Application of a conceptual runoff model in different physiographic regions of Switzerland. *Hydrological sciences journal*, **37,** 217-231.

Braun, L. N., E. Brun, Y. Durand, E. Martin, and P. Tourasse, 1994: Simulation of discharge using different methods of meteorological data distribution, basin discretization and snow modelling. *Nordic Hydrology*, **25,** 129-144.

Breiling, M. and P. Charamza, 1999: The impact of global warming on winter tourism and skiing: a regionalised model for Austrian snow conditions. *Regional Environmental Change*, **1,** 4-14.

Briffa, K. R. and P. D. Jones, 1993: Global surface air temperature variations during the twentieth century: Part 2, implications for large-scale high-frequency paleoclimatic studies. *The Holocene*, **3,** 77-88.

Buishand, T.A., Shabalova, M.V. and Brandsma, T., 2004: On the choice of the temporal aggregation level for statistical downscaling of precipitation. *Journal of Climate*, **17,** 1816–1827.

Bultot, F., D. Gellens, M. Spreafico, and B. Schädler, 1992: Repercussions of a CO2 doubling on the water balance - a case study in Switzerland. *Journal of Hydrology*, **137,** 199-208.

Bultot, F., D. Gellens, B. Schädler, and M. Spreafico, 1994: Effects of climate change on snow accumulation and melting in the Broye catchment (Switzerland). *Climatic Change*, **28,** 339-363.

Bürki, R., 2000: Klimaänderung und Anpassungsprozesse im Wintertourismus (Climate change and adaptation processes in winter tourism). Ostschweizerische Geographische Gesellschaft, St. Gallen, 206 pp.

Charles, S. P., B. C. Bates, P. H. Whetton, and J. P. Hughes, 1999: Validation of downscaling models for changed climate conditions: case study of southwestern Australia. *Climate Research*, **12,** 1-14.

Cubasch, U., K. Hasselmann, H. Höck, E. Maier-Reimer, U. Mikolajewicz, B. D. Santer, and R. Sausen, 1992: Time-dependent greenhouse warming computations with a coupled ocean-atmosphere model. *Climate Dynamics*, **8,** 55-69.

Cubasch, U., G. A. Meehl, G. J. Boer, R. J. Stouffer, M. Dix, A. Noda, C. A. Senior, S. Raper, and K. S. Yap, 2001: Projections of future climate change. *Climate change 2001: The scientific basis. Contribution of working group I to the third assessment report of the Intergovernmental Panel on Climate Change*, J. T. Houghton, Y. Ding, D. J. Griggs, M. Noguer, P. J. van der Linden, X. Dai, K. Maskell, and C. A. Johnson, Eds., Cambridge University Press, 525-582.

Ehrler, C., 1998: Klimaänderung und alpine Schneedecke - Auswirkungen auf das Abflussregime am Beispiel des Einzugsgebiets Rhein-Felsberg (Climate change and the alpine snow cover - Consequences for the runoff regime using the Rhein-Felsberg catchment as an example). vdf Hochschulverlag an der ETH, 134 pp.

Etchevers, P., Martin, E., Brown, R., Fierz, C., Lejeune, Y., Bazile, E., Boone, A., Dai, Y.-J., Essery, R., Fernandez, A., Gusev, Y., Jordan, R., Koren, V., Kowalczyk, E., Nasonova, N.O., Pyles, R.D., Schlosser, A., Shmakin, A.B., Smirnova, T.G., Strasser, U., Verseghy, D., Yamazaki, T. & Yan, Z.-L. (2004). Validation of the energy budget of an alpine snowpack simulated by several snow models (SNOWMIP project). Ann. Glaciol. **38,** 150-158.

Essery, R., E. Martin, H. Douville, A. Fernandez, and E. Brun, 1999: A comparison of four snow models using observations from an alpine site. *Climate Dynamics*, **15,** 583-593.

Fischlin, A. and D. Gyalistras, 1997: Assessing impacts of climatic change on forests in the Alps. *Global Ecology and Biogeography Letters*, **6,** 19-37.

Föhn, P., 1990: Schnee und Lawinen (Snow and avalanches). *Schnee, Eis und Wasser der Alpen in einer wärmeren Atmosphäre*, Zurich, Versuchsanstalt für Wasserbau, Hydrologie und Glaziologie der ETH Zürich, 33-48.

Gates, W. L., A. Henderson-Sellers, G. J. Boer, C. K. Folland, A. Kitoh, B. J. McAvaney, F. Semazzi, N. Smith, A. J. Weaver, and Q.-C. Zeng, 1996: Climate models - evaluation. *Climate Change 1995: The Science of Climate Change. Contribution of Working Group I to the Second Assessment Report of the Intergovernmental Panel on Climate Change*, J. T. Houghton, L. G. Meira Filho, B. A. Callander, N. Harris, A. Kattenberg, and K. Maskell, Eds., Cambridge University Press, 229-284.

Giorgi, F., J. W. Hurrell, M. R. Marinucci, and M. Beniston, 1997: Elevation dependency of the surface climate change signal: a model study. *Journal of Climate*, **10,** 288-296.

Gyalistras, D., Fischlin, A. & Riedo, M. 1997. Herleitung stündlicher Wetterszenarien unter zukünftigen Klimabedingungen. In: Fuhrer, J. (ed.), *Klimaänderung und Grünland - eine Modellstudie über die Auswirkungen einer Klimaänderung auf das Dauergrünland in der Schweiz*. vdf, Hochschulverlag AG an der ETH Zürich, pp. 207-276.

Gyalistras, D. and A. Fischlin, 1999: Towards a general method to construct regional climatic scenarios for model-based impacts assessments. *Petermanns geographische Mitteilungen*, **143,** 251-264.

Gyalistras, D., H. von Storch, A. Fischlin, and M. Beniston, 1994: Linking GCM-simulated climatic changes to ecosystem models: case studies of statistical downscaling in the Alps. *Climate Research*, **4,** 167-189.

Gyalistras, D., C. Schär, H. C. Davies, and H. Wanner, 1998: Future Alpine climate. *Views from the Alps: regional perspectives on climate change*, P. Cebon, U. Dahinden, H. C. Davies, D. Imboden, and C. Jäger, Eds., MIT Press, 171-223.

Hantel, M., M. Ehrendorfer, and A. Haslinger, 2000: Climate sensitivity of snow cover duration in Austria. *International Journal of Climatology*, **20,** 615-640.

Harrison, J., Winterbottom, S. & Johnson, R., 2001: Climate change and changing snowfall patterns in Scotland. The Scottish Executive Central Research Unit, Edinburgh, 48pp.

Jaagus, J., 1997: The impact of climate change on the snow cover pattern in Estonia. *Climatic Change*, **36,** 65-77.

Jasper, K., Calanca, P., Gyalistras, D. & Fuhrer, J., 2004: Differential impacts of climate change on the hydrology of two alpine river basins. *Clim. Res.*, **26,** 113-129.

Jones, P. D. and K. R. Briffa, 1992: Global surface air temperature variations during the twentieth century: Part 1, spatial, temporal and seasonal details. *The Holocene*, **2,** 165-179.

Jones, P.D. & Moberg, A. (2003). Hemispheric and large-scale surface air temperature variations: An extensive revision and an update to 2001. *J. Clim.*, **16,** 206–223.

Kleinn, J., 2002: Climate change and runoff statistics in the Rhine Basin: a process study with a coupled climate-runoff model, Swiss Federal Institute of Technology (ETH), 114.

Koch, E. and E. Rudel, 1990: Mögliche Auswirkungen eines verstärkten Treibhauseffektes auf die Schneeverhältnisse in Österreich (Possible consequences of an enhanced greenhouse effect on snow conditions in Austria). *Wetter und Leben*, **45,** 137-153.

Laternser, M. and M. Schneebeli, 2003: Long-term snow climate trends of the Swiss Alps (1931-99). *International Journal of Climatology*, **23,** 733-750.

Leung, L. R., Y. Qian, X. Bian, W. M. Washington, J. Han, and J. O. Roads, 2004: Mid-century ensemble regional climate change scenarios for the western united states. *Climatic Change*, **62,** 75-113.

Martin, E., Brun, E. & Durand, Y., 1994: Sensitivity of the French Alps snow cover to the variation of climatic variables. *Ann. Geophys.*, **12**, 469-477.

Martin, E., B. Timbal, and E. Brun, 1997: Downscaling of general circulation model outputs: simulation of the snow climatology of the French Alps and sensitivity to climate change. *Climate Dynamics*, **13,** 45-56.

Martinec, J., 1977: Expected snow loads on structures from incomplete hydrological data. *The Journal of Glaciology*, **19,** 185-195.

Mavromatis, T. & Hansen, J.W., 2001: Interannual variability characteristics and simulated crop response of four stochastic weather generators. Agric. For. Meteorol. **109,** 283-296.

McFarlane, N. A., G. J. Boer, J.-P. Blanchet, and M. Lazare, 1992: The Canadian Climate Centre second-generation general circulation model and its equilibrium climate. *Journal of Climate*, **5,** 1013-1044.

Mearns, L. O., M. Hulme, T. R. Carter, R. Leemans, M. Lal, and P. Whetton, 2001: Climate scenario development. *Climate change 2001: The scientific basis. Contribution of working group I to the third assessment report of the Intergovernmental Panel on Climate Change*, J. T. Houghton, Y. Ding, D. J. Griggs, M. Noguer, P. J. van der Linden, X. Dai, K. Maskell, and C. A. Johnson, Eds., Cambridge University Press, 739-768.

Monro, J. C., 1971: Direct search optimization in mathematical modelling and a watershed application. NOAA Technical Memorandum NWS HYDRO, 52 pp.

Riedo, M., D. Gyalistras, A. Fischlin, and J. Fuhrer, 1999: Using an ecosystem model linked to GCM-derived local weather scenarios to analyse effects of climate change and elevated CO2 on dry matter production and partitioning, and water use in temperate managed grasslands. *Global Change Biology*, **5,** 213-223.

Riedo, M., D. Gyalistras, A. Grub, M. Rosset, and J. Fuhrer, 1997: Modelling grassland responses to climate change and elevated CO2. *Acta Oecologica Applicata*, **18,** 305-311.

Rohrer, M. B., 1989: Determination of the transition air temperature and intensity of precipitation. Instruments and Observing Methods Report No. 48, 475-482 pp.

——, 1992: Die Schneedecke im Schweizer Alpenraum und ihre Modellierung. Analyse langjähriger Schneemessungen und Modellierung des Wasseräquivalentes aufgrund zeitlich hoch aufgelöster operationell gemessener meteorologischer Daten. (The snow cover of the Swiss Alps and its modelling. Analysis of long-term measurements and modelling of the water equivalent based on temporally highly resolved, operationally measured meteorological data.). Zürcher Geographische Schriften, 178 pp.

Rohrer, M. B., L. N. Braun, and H. Lang, 1994: Long-term records of snow cover water equivalent in the Swiss Alps: 1. Analysis. *Nordic Hydrology*, **25,** 53-64.

Scherrer, S. C., Appenzeller, C. & Laternser, M. (2004). Trends in Swiss Alpine snow days: The role of local- and large-scale climate variability. Geophys. Res. Lett., 31, L13215, doi:10.1029/2004GL020255.

Schulla, J., 1997: Hydrologische Modellierung von Flussgebieten zur Abschätzung der Folgen von Klimaänderungen (Hydrological modelling of river basins for the assessment of climate change impacts). Zürcher Geographische Schriften, 187 pp.

Scott, D., Jones, B., Lemieux, C., McBoyle, G., Mills, B., Svenson, S. & Wall, G., 2002: The vulnerability of winter recreation to climate change in Ontario's Lakelands Tourism Region. Occasional Paper 18, Department of Geography Publication Series, University of Waterloo, Waterloo, Canada, 84 pp.

Scott, D., G. McBoyle, and B. Mills, 2003: Climate change and the skiing industry in southern Ontario (Canada): exploring the importance of snowmaking as a technical adaptation. *Climate Research*, **23,** 171-181.

Seidel, K., Ehrler, C. & Martinec, J., 1998. Effects of climate change on water resources and runoff in an Alpine basin. *Hydrol. Processes*, **12**, 1659-1669.

Semádeni-Davies, A., 1997: Monthly snowmelt modelling for large-scale climate change studies using the degree day approach. *Ecological Modelling*, **101,** 303-323.

Semenov, M. A., R. J. Brooks, E. M. Barrow, and C. W. Richardson, 1998: Comparison of the WGEN and LARS-WG stochastic weather generators for diverse climates. *Climate Research*, **10,** 95-107.

Sevruk, B. 1985: Systematischer Niederschlagsmessfehler in der Schweiz. In: Sevruk, B. (ed) Der Niederschlag in der Schweiz. Beitr. Geol. Schweiz. Hydrol. **31**, 65–75.

Stadler, D., M. Bründl, M. Schneebeli, M. Meyer-Grass, and H. Flühler, 1998: *Hydrologische Prozesse im subalpinen Wald im Winter (Hydrological processes in the subalpine forest during wintertime)*. vdf Hochschulverlag an der ETH, 145 pp.

Trenberth, K. E. and D. A. Paolino Jr., 1980: The Northern Hemisphere sea-level pressure data set: Trends, errors and discontinuities. *Monthly Weather Review*, **108,** 855-872.

von Storch, H., 1995: Inconsistencies at the interface of climate impact studies and global climate research. *Meteorologische Zeitschrift*, **4,** 72-80.

von Storch, J.-S., V. Kharin, U. Cubasch, G. Hegerl, D. Schriever, H. von Storch, and E. Zorita, 1997: A description of a 1260-year control integration with the coupled ECHAM1/LSG general circulation model. *Journal of Climate*, **10,** 1525-1543.

von Storch, H. and F. W. Zwiers, 1999: Statistical analysis in climate research. Cambridge University Press, 484.

von Storch, H., 1999: On the use of inflation in statistical downscaling. *Journal of Climate*, **12,** 3505-3506.

Wanner, H., D. Gyalistras, J. Luterbacher, R. Rickli, E. Salvisberg, and C. Schmutz, 2000: *Klimawandel im Schweizer Alpenraum (Climate change in the Swiss Alps)*. vdf, Hochschulverlag AG an der ETH Zürich, 285 pp.

Whetton, P. H., M. R. Haylock, and R. Galloway, 1996: Climate change and snow-cover duration in the Australian Alps. *Climatic Change*, **32,** 447-479.

Widmann, M. and C. S. Bretherton, 2000: Validation of mesoscale precipitation in the NCEP reanalysis using a new gridpoint data set for the northwestern US. *Journal of Climate*, **13,** 1936-1950.

Wielke, L.-M., Haimberger, L. & Hantel, M., 2004: Snow cover duration in Switzerland compared to Austria. Meteorol. Z., **13,** 13-17.

Witmer, U., 1986: Erfassung, Bearbeitung und Kartierung von Schneedaten in der Schweiz (Registration, processing and mapping of snow data in Switzerland). Geographica Bernensia, Series G (Basic Research) 3-906290-28-X, 215 pp.

WMO, 1986: Intercomparison of models of snowmelt runoff. Operational hydrology report No. 23 92-63-10646-0, xxxii + 440 pp.